



Long-Term Monitoring of Cloud Water Chemistry at Whiteface Mountain: The Emergence of a New Chemical Regime

Christopher E. Lawrence¹, Paul Casson¹, Richard Brandt¹, James J. Schwab¹, James E. Dukett², Phil Snyder², Elizabeth Yerger³, Daniel Kelting³, Trevor C. VandenBoer⁴, and Sara Lance¹

¹Atmospheric Sciences Research Center (ASRC), University at Albany, SUNY ETEC building, 1220 Washington Ave, Albany NY 12226

²Adirondack Lake Survey Corporation (ALSC), 1115 NYS Rt.86, P.O. BOX 296, Ray Brook NY 12977

³Paul Smith's College Adirondack Watershed Institute (AWI), P. O. Box 265, Routes 86 and 30, Paul Smiths NY 12970

⁴Department of Chemistry, York University, Toronto, Ontario, Canada

Correspondence: Sara Lance (smlance@albany.edu)

Abstract.

Atmospheric aqueous chemistry can have profound effects on our environment. The importance of chemistry within the atmospheric aqueous phase was first realized in the 1970s as there was growing concern over the negative impacts on ecosystem health from acid deposition. Research at mountaintop observatories including Whiteface Mountain (WFM) showed that gas phase sulfur dioxide emissions react in cloud droplets to form sulfuric acid, which also impacted aerosol mass loadings. Cloud chemistry research has experienced a major resurgence in scientific interest due to the potential for aqueous chemical processes to fill the gap between modeled and observed organic aerosol mass.

The current study updates the long-term trends in cloud water composition at WFM for the past 28 years (1994-2021). Substantial decreases in sulfate (SO_4^{2-}) and nitrate (NO_3^-) concentrations have not been matched by an equivalent decrease in ammonium (NH_4^+) concentrations, leading to significantly higher cloud droplet pH. Meanwhile, Total Organic Carbon (TOC) concentrations may be increasing (both in relative and absolute terms). In the past, samples were excluded from trend analysis if they did not meet an approximate ion balance, which resulted in approximately half of samples being excluded in recent years. We show that, when including the entire available dataset, decreasing trends in SO_4^{2-} , NO_3^- , and NH_4^+ become more modest, TOC concentrations increase at a faster rate, and increasing trends in Ca^{2+} and Mg^{2+} emerge. A growing trend in cation/anion ratios is also observed, implying that a significant fraction of anions are not being measured with the current suite of measurements, and these missing anions are growing in importance. Organic acids are identified as the most likely candidates for the missing anions, since the measured ion imbalance correlates strongly with measured TOC concentrations. The TOC trend becomes statistically insignificant when evaluating cloud water loadings (or air equivalent mass loadings), possibly due to the complex role that LWC may play in TOC concentrations. We highlight the emergence of a new chemical regime characterized by low acidity and relatively high conductivity, and increasing TOC and base cation concentrations. With the increasing impact from Ca^{2+} and Mg^{2+} on the bulk cloud water pH, which are largely thought to reside within coarse mode aerosol that only represent a small fraction of cloud droplets, an "inferred cloud droplet pH" is introduced, to better represent the pH of the vast majority of cloud droplets as they reside in the atmosphere. While measured pH has increased



during the history of the monitoring site, the cloud droplet pH has remained relatively flat since 2009. We also show that there
25 is a missing source of acidity in the system that correlates with TOC. The chemical system at WFM has shifted away from a
system dominated by SO_4^{2-} to a system controlled by base cation, nitrogen containing species and TOC. Further research is
required to understand the effects on air quality, climate, and ecosystem health.

1 Introduction

Whiteface Mountain (WFM) has been an important site for cloud water chemistry measurements dating back to the 1980s
30 (Falconer and Falconer, 1980; Mohnen and Vong, 1993), while routine summertime cloud water monitoring began in 1994.
Much of the interest in cloud chemistry developed as a result of increasing emissions of sulfur dioxide (SO_2) and nitrogen
oxides (NO_x) in the second half of the 20th century. Through field experiments at WFM and other locations in the Eastern
U.S., researchers established that these gases, originating largely from fossil fuel combustion, can dissolve in cloud droplets
and undergo photochemical formation of sulfate (SO_4^{2-}) and nitrate (NO_3^-). This chemistry has contributed substantially to
35 particulate mass, posing significant health risks and contributing to cooling effects on the climate (Kiehl and Briegleb, 1993;
Pope and Dockery, 2006; Myhre et al., 2013). SO_4^{2-} and NO_3^- are also the major causes behind acid deposition, a process that
can have detrimental ecosystem effects such as decreased aquatic biodiversity, calcium depletion from soils, release of toxic
aluminum (Gorham, 1998) and deterioration of building material (Xie et al., 2004). These growing societal and environmental
problems helped influence and shape amendments to the Clean Air Act in the 1990s focusing on the criteria air pollutants (SO_2
40 and NO_x). In addition to these emission reductions, the U.S. Environmental Protection Agency (EPA) formed a network of
the mountaintop sites in the Eastern U.S. through the Mountain Acid Deposition Program (MADPro) to monitor the progress
of Clean Air Act Amendments. The regulation of these emissions proved to be successful, as SO_2 and to a lesser extent NO_x
have decreased for several decades in the U.S. (US EPA, 2019), leading to decreases in the acid deposition throughout the
Eastern U.S., including New York State (Rattigan et al., 2017). Substantial decreases in cloud water acidity were also observed
45 at WFM, corresponding to both decreases in cloud water acidity and particulate matter (PM 2.5) concentrations of SO_4^{2-} and,
more modestly, NO_3^- (Schwab et al., 2016b). Many ecosystems in the Adirondacks previously impacted by acid deposition
have shown signs of recovery (Driscoll et al., 2016).

The significant reductions in SO_4^{2-} and NO_3^- , and therefore cloud water acidity, indicate a dramatically changed chemical
system, with a growing contribution from less well-understood and more labile analytes such as organic carbon and ammo-
50 nium (NH_4^+). Organic carbon is found ubiquitously throughout the atmosphere, playing key roles in ozone formation and
aerosol physicochemical properties such as hygroscopicity, optical properties and reactivity (Jimenez et al., 2009). During a
two-week pilot study at WFM in 2017, organic matter was shown to comprise as much as 93%, and an average of 78%, of
submicron aerosol mass (Zhang et al., 2019). Similarly, total organic carbon (TOC), the sum of particulate and dissolved OC,
is an important component within cloud and fog droplets (Herckes et al., 2013). Organic compounds are chemically complex,
55 containing 1000s of compounds, all with different chemical and physical properties spanning orders of magnitude in volatility
and solubility, which dictates the chemical pathways they can take part in (Jimenez et al., 2009), making their identification and



potential environmental effects challenging to determine (Herckes et al., 2013). The controlling factors for TOC concentrations in cloud droplets are highly uncertain. Organic compounds can also interact with inorganic ions within cloud droplets to form compounds like organic salts, organic nitrogen, and organic sulfur compounds (McNeill, 2015).

60 Reactive nitrogen deposition, from both reduced and oxidized forms, has also been gaining increased attention (Kanakidou et al., 2016; Stevens et al., 2018). While nitrogen can act as a nutrient in ecosystems that are nitrogen limited, excess deposition can lead to harmful environmental effects such as soil acidification by leaching out buffering base cations like calcium (Ca^{2+}), magnesium (Mg^{2+}) and potassium (K^+), and through nitrification, potentially mobilizing toxic metals such as aluminum (Lawrence and David, 1997; Tian and Niu, 2015). Nitrogen deposition, when combined with other factors, can also contribute
65 to harmful algal blooms which threaten aquatic ecosystems and human health (Paerl and Otten, 2013). A significant fraction of total nitrogen (TN) in cloud and rain water is organic nitrogen (ON), typically comprising $\sim 30\%$ of water soluble nitrogen (Cape et al., 2011). Much like organic carbon, the sources of organic nitrogen, as well as the chemical aging, deposition, and ecosystem effects, are highly uncertain and require more research. Ammonia (NH_3) is the primary atmospheric base in Earth's atmosphere, and an unregulated gas phase pollutant with increasingly recognized importance to atmospheric chemistry. Despite
70 emissions of NH_3 in the U.S. largely decreasing prior to 2015 (US EPA, 2019), since then atmospheric concentrations of NH_3 appear to be increasing (Warner et al., 2017; Liu et al., 2019). At the same time, aerosol NH_4^+ concentrations have steadily decreased and wet precipitation NH_4^+ concentrations have remained relatively constant (Rattigan et al., 2017), suggesting that complex long-term shifts in NH_3 partitioning are taking place.

This paper provides an updated review of trends in summertime cloud water composition at WFM using data obtained
75 from MADPro (1994-2000), the long-term monitoring conducted by the Adirondack Lake Survey Corporation (ALSC) (2001-2017) and recent measurements conducted under the oversight of the Lance Lab at the Atmospheric Sciences Research Center (ASRC) (2018-2021). A detailed review of the sample collection methods and laboratory analyses over this period are also discussed, with a focus on major system changes that have not been fully described in previously published scientific papers. Previous works have reported trends in bulk cloud water composition at WFM up to 2013, largely focusing on analytes most
80 relevant for acid deposition (Aleksic et al., 2009; Dukett et al., 2011; Schwab et al., 2016b). Here, a critical review of past data analysis methodologies is presented, alongside a thorough assessment and justification for modifications to these methodologies, which have resulted in significant changes to the long-term trends. In this paper, we also report the first long-term trends in cloud water TOC at WFM, along with additional analysis of NH_4^+ and non-volatile cation concentrations (Ca^{2+} , Mg^{2+} , K^+) in cloud water.

85 2 Collection History, Methods, Laboratory Procedure, and Data Analysis

2.1 Site Description and Collection Methods

Whiteface Mountain (WFM) is located in the “High Peaks” Region of the Adirondacks Mountains in Upstate, NY, with summit elevation of 1483m. The WFM site history is described in detail by (Schwab et al., 2016a, b). It should be noted that the first cloud water TOC measurements at WFM were conducted for a handful of cloud events in 1987, along with the only published

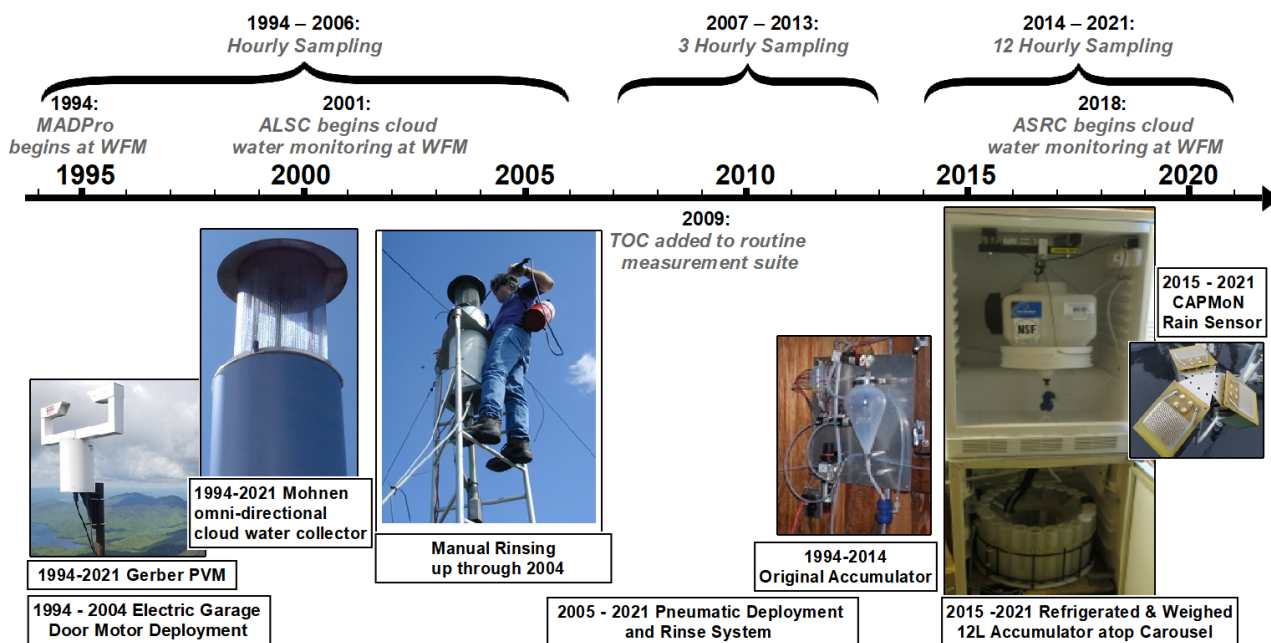


Figure 1. Timeline of major events in cloud water collection at WFM for the data set analyzed in this paper (1994-2021), with sampling conducted by the Mountain Acid Deposition Program (MADPro) 1994-2000, the Adirondack Lake Survey Corporation (ALSC) 2001-2017, and the Atmospheric Sciences Research Center (ASRC) 2018-2021, and two major system overhauls in 2005 and in 2015. The same basic protocols, cloud water collector and liquid water content sensor were used throughout this entire measurement period, but sampling frequency decreased from hourly to 3-hourly to 12-hourly, necessitating a larger accumulator vessel and an additional refrigerator to house it. Automated filtering began in 2018. Photos documenting the manual rinsing process and the original accumulator were obtained from Eric Hebert, Environmental Engineering Measurement Services, Inc.

90 organic acid measurements in cloud water at WFM to date. This powerful seminal study showed that potential sources of organic carbon including organic acids could share similar sources with SO_4^{2-} and NO_3^- (Khwaja et al., 1995). Water Soluble Organic Carbon (WSOC) measurements were also previously obtained for a selection of cloud water samples at WFM from 1990 to 1992 (Anastasio et al., 1994).

All of the bulk cloud water data reported in this paper used a Mohnen omni-directional passive cloud water collector (Mohnen, 1980)(Fig. 1). The collector contains two disks with 0.035-0.04mm Teflon strings strung vertically between the disks. As cloud droplets pass through the collector and collide with the Teflon strings, water beads up and eventually drips down the strings. The cloud water is then funneled by gravity through a tube and fed into a high density polyethylene vessel called an accumulator. The accumulator then dumps into 1 liter sample bottles contained in a carousel within a refrigerator below the accumulator.

100 Deployment of the collector was automated starting in 1994 during the MADPro campaign, and, since that time, the following meteorological parameters have been used to trigger deployment of the collector: 1) liquid water content (LWC) is > 0.05

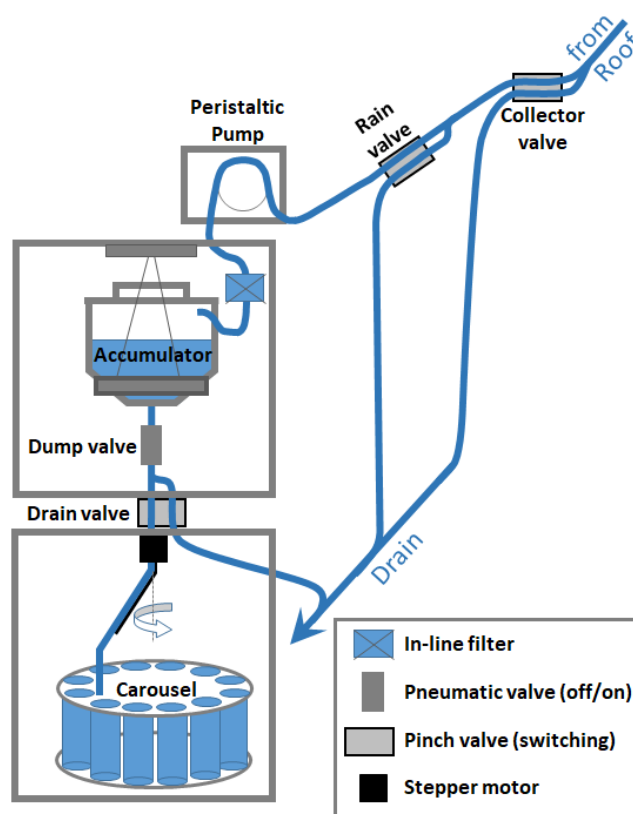


Figure 2. Schematic of the physical components of the current cloud water collection system inside the research observatory at the summit of WFM. A series of valves control where the collected cloud water is directed at specific times, with multiple opportunities to be directed to a waste stream marked 'Drain'. Up to 1 liter is collected in each bottle within the carousel. The two refrigerated parts of the system house the Accumulator and the Carousel, where the sample is stored for up to 3 days before delivery to an analytical laboratory for analysis.

g m⁻³ measured by a Gerber Particle Volume (PVM) (Gerber, 1991), indicating the presence of a cloud. (Seinfeld and Pandis, 2016), 2) temperature is above 2°C to prevent damage to the collector from riming, 3) rain is not detected, to limit measurements to non-precipitating clouds. Rain was detected using an Aerochem gridded rain sensor from 1994 to 2014, which was
105 updated in 2015 to a CAPMoN heated grid rain sensor (Mekis et al., 2018), 4) and lastly, wind-speed is > 2 m s⁻¹, allowing cloudy air to pass through the collector, measured using a RM Young anemometer. If all of these meteorological parameters are met, the collector is raised from its protective housing, exposing the Teflon strings to the passing airflow. Figure 1 summarizes the major events and changes to the cloud collection at WFM.

The automated collection system originally deployed the cloud water collector using an electric garage door opener motor,
110 which was upgraded in 2005 to a pneumatic system to increase deployment and retraction speed. A pressurized tank of deionized water also replaced the manual electric pump spray system in 2005. To monitor for potential contamination, blanks and



rinses of the cloud collector were obtained regularly throughout each summer and assessed for the same analytes as the cloud water samples. The collector was rinsed with deionized water for at least 15 seconds between samples, except when sample changes occurred while deployed in cloud.

115 Cloud water samples were refrigerated at temperatures that never exceed 4 °C for up to 3 days within the carousel refrigerator and then transported to a laboratory for subsequent chemical analysis. From 1994-2006, the accumulator dumped into a sample bottle every hour and the carousel advanced to the next bottle. Starting in 2007, samples were dumped every hour and later pooled together into 3 hour composite samples prior to analysis. In 2014, the one hour samples were pooled together into 12
120 hour composite samples. Then, starting in 2015, the 1 liter accumulator was replaced with a 12 liter accumulator to accumulate cloud water over 12 hour periods, providing up to one daytime and one nighttime sample per day. The new 12 liter accumulator was housed in a separate refrigerator above the carousel refrigerator to prevent microbial degradation of the sample prior to freezing the sample, and a measurement of the accumulator weight was added to continuously monitor the volume of cloud water collected.

Control of the cloud water collection system is accomplished through four pinch valves, three of which divert the sample
125 stream one of two ways under different conditions, and a pneumatic ‘Dump valve’ to effectively stop flow out of the accumulator. The ‘Collector valve’ diverts flow to waste whenever the collector is not actively deployed. The ‘Drain valve’ diverts flow to waste after 1 liter has been collected in sample bottles within the carousel (since bottles in the carousel can only hold 1 liter). The ‘Rain valve’ operates at a higher frequency than the 1 minute timescale of the ‘Collector valve’ and diverts flow to waste when the rain sensor detects rain but the collector has not yet retracted back into its housing.

130 Starting in 2018, an automated filtering system with in-line peristaltic pump was added just prior to the accumulator (Fig. 2), to prevent potential microbial degradation of the sample. This change in protocol was introduced to safeguard samples for subsequent analysis of the organic constituents, since organics now comprise a major fraction of aerosol and cloud water solute mass, and their chemical and physical properties remain poorly understood. Automated filtering could be important for preserving some organic compounds for up to 3 days within the carousel refrigerator, since some microbes are known to both
135 consume and produce organic compounds even at temperatures as low as 0 °C (Van Stempvoort and Biggar, 2008). For the first year of automated filtering, only a few samples were filtered during collection, and field tests were conducted to verify that the filter used did not introduce measurement artifacts. It should be noted that after automated filtering commenced, TOC could no longer be measured as the filtration removes particulate organic carbon, and instead measurements of water soluble organic carbon (WSOC) were obtained. To estimate the fraction of TOC no longer being measured due to this change in protocol,
140 both TOC and WSOC were measured for a subset of samples in 2018 and 2019 (Fig. S1). The comparison between WSOC and TOC for these samples yielded on average 15% insoluble organic carbon, within the range reported in previous studies (typically between 6 and 23%) (Herckes et al., 2013).

As used by Khwaja et al. (1995), a pre-washed 0.4 μm track-etched polycarbonate filter was selected, balancing the need for microbial removal and the need for low enough pressure drop to attain reliable operation of the automated filtering apparatus.
145 The in-line filter was housed within the accumulator refrigerator to prevent microbial growth on the filter substrate. Since pressures in excess of 40 psig could occur under high particulate load on the filter, PTFE reinforced silicone peristaltic pump



tubing (GORE STA-PURE PCS) was used to prevent tubing rupture, and filters were replaced during every site visit, nominally every 3 days. The peristaltic pump was also triggered to only turn on during cloud events when the collector was deployed, to prevent unnecessary wear and tear on the peristaltic pump tubing.

150 2.2 Chemical Analysis and Data Handling

The list of routinely measured analytes for this long-term dataset is: conductivity, pH, SO_4^{2-} , NO_3^- , NH_4^+ , Cl^- , Na^+ , Ca^{2+} , Mg^{2+} , and K^+ , with TOC measurements beginning in 2009. MADPro and ALSC measured each ion using similar methods recommended by the U.S. EPA. For anions, ion chromatography was conducted according to the EPA 300.1 method. MADPro used Dionex instruments throughout the campaign. From 2005 until 2014, ALSC used a Thermo Scientific Dionex ICS-
155 600 Ion Chromatography system. In July 2014, the system was replaced with a Thermo Scientific Dionex ICS-1100 Ion Chromatography system. For 2018 and 2019, cloud water composition was measured at AWI. SO_4^{2-} and Cl^- were measured via ion chromatography using a Lachat QC 8500 Ion Chromatograph. There is likely a high bias for the Cl^- data for 2018 and 2019, as there were issues with detection limits. A cadmium reduction technique couple with Lachat QC 8500 Flow Injection Analyzer was used to measure NO_3^- , as described by the EPA 352.2 method. This technique was used as NO_3^- was co-eluting
160 with other peaks within the chromatograms, making identification by ion chromatography not possible. It should be noted that cadmium reduction measures both NO_2^- and NO_3^- , potentially biasing NO_3^- high. However, NO_2^- is expected to exist in negligible concentrations in comparison to NO_3^- and therefore likely not impacting the measurement significantly. Metals were measured using a Inductively Coupled Plasma-Atomic Emissions Spectrometry analyzer, following the EPA 200.7 method. For cations, MADPro used Perkin-Elmer P-2 inductively coupled argon plasma (ICAP) atomic emission spectrometer to measure
165 Ca^{2+} , Mg^{2+} , and Na^+ . In 1994, K^+ was measured using a flame atomic emission spectrometry, and switched to ICAP atomic emissions for the remainder of the project. MADPro used a Perkin-Elmer P-2 ICAP atomic emissions spectrometer. Between the years 2000 to 2014, ALSC used a Perkin Elmer analyst 300 Flame/Graphite furnace Atomic Absorption Spectrometer (AAS) to measure Ca^{2+} , Mg^{2+} , K^+ , and Na^+ , which was replaced in September 2014 with a Perkin Elmer Pinnacle 900H Flame Graphite Furnace AAS. Both MADPro and ALSC used an automated phenolate method combined with colorimetry
170 for NH_4^+ analysis according to the EPA 350.1 method (EPA, 1983). Both MADPro and ALSC categorized data based on ion balance criteria according to the relative percent difference (RPD) between the measured cation and anion concentrations, calculated as follows:

$$\text{RPD} = 100\% * \frac{\sum \text{Cations} - \sum \text{Anions}}{(\sum \text{Cations} + \sum \text{Anions})/2} \quad (1)$$

Samples were categorized as Valid based on RPD using the following thresholds: $\text{RPD} < 100\%$ when both $\sum \text{Cations}$ and
175 $\sum \text{Anions} < 100 \mu\text{eq L}^{-1}$, or $\text{RPD} < 25\%$ when either $\sum \text{Cations}$ or $\sum \text{Anions} > 100 \mu\text{eq L}^{-1}$. Samples that did not match these criteria were considered Invalid. Samples with flagged data due to suspected measurement problems were also considered Invalid, which were extremely rare, only representing $< 1\%$ of samples. Samples for which all analytes could not be measured (for instance, due to insufficient sample volume) were omitted from our separate analysis of Invalid and Valid datasets, and



we refer to these samples as Unclassified since ion balance could not be fully assessed for these samples. Fewer than 10%
180 of samples were Unclassified. Previous analyses involving the MADPro and ALSC data sets typically only used Valid data
(i.e. those samples that passed the ion balance criteria and were also not subject to any known or suspected measurement
problems), which has important implications for the data interpretation and the resulting long-term trends, as will be discussed
in the results section of this work.

TOC was measured according to the EPA 450.1 method using a Tekmar Dorhmann Phoenix 800 Carbon Analyzer from 2009
185 to 2015. In April 2015, the system was replaced with a Teledyne Tekmar TOC Fusion Carbon Analyzer. Lastly, WSOC was
measured using a Shimadzu TOC-VCPN Total Organic Carbon Analyzer. In 2020 and 2021, chemical analysis were done by
ALSC, using the same methods described above. Accuracy measurements was determined using prepared reference standards
and were run every 10 cloud samples. Each year, 5-10 split samples were sent to another analytical lab to measure the same
suite of analytes as an additional quality control measure.

190 Previous studies also often focused on reporting sample volume-weighted analyte concentrations due to a focus on wet
deposition, whereas we report measured cloud water concentrations and cloud water loadings, the latter of which complements
measurements of aerosol loadings. Since a typical cloud droplet is more likely to evaporate than deposit to the surface at any
given time (Seinfeld and Pandis, 2016), this latter focus on atmospheric loadings is useful for investigating chemical processes
occurring in the atmosphere separately from the influence of sample dilution at higher LWC.

195 To account for variability in LWC that potentially affected cloud water concentrations, cloud water loadings (CWL) are
calculated as follows (Elbert et al., 2000; Marinoni et al., 2004; Kim et al., 2019):

$$CWL = \frac{LWC_{\text{samp}} * [X_i] * mw_i}{\rho_w * Z_i} \quad (2)$$

where CWL is expressed in μg solute per m^3 of air, LWC_{samp} is the representative LWC during which the sample was
collected expressed in g water per m^3 of air, $[X_i]$ is the liquid concentration of a given solute ion i expressed in μeq solute per
200 L of water, mw_i is the molecular weight of the solute in g mol^{-1} , Z_i is the solute charge and ρ_w is the density of cloud water
(assumed to be 1 g cm^{-3}). To calculate TOC CWL, $[X_i]/Z_i$ is replaced with molar concentration in $\mu\text{mol C per L}$ and mw_i
 $= 12 \text{ g mol}^{-1}$. While the long-term WFM data set included average LWC values for each sample, there is no record of how
these values were determined, and careful analysis indicates that these values included LWC values during periods with drizzle
when collected cloud water was being sent to a waste stream and the collector is not deployed, a common occurrence during
205 the night. To avoid introducing bias into the CWL calculation, we recalculated LWC_{samp} by removing LWC values from the
average when the rain sensor detected rain for $> 15\%$ of a given measurement period or the collector is deployed for the less $<$
 25% of a measurement period as described in the supplemental material (Fig. S2). Since this additional information about the
collector status and meteorological conditions during each hour is only available starting in 2009, only data from 2009 to 2021
is included in our LWC_{samp} and CWL calculations.

210 In the present study, data analysis is performed within the statistical software R (Team, 2021). Measured analyte concen-
trations and conductivity exhibit a log-normal distributions, therefore median values were used rather than means for trend

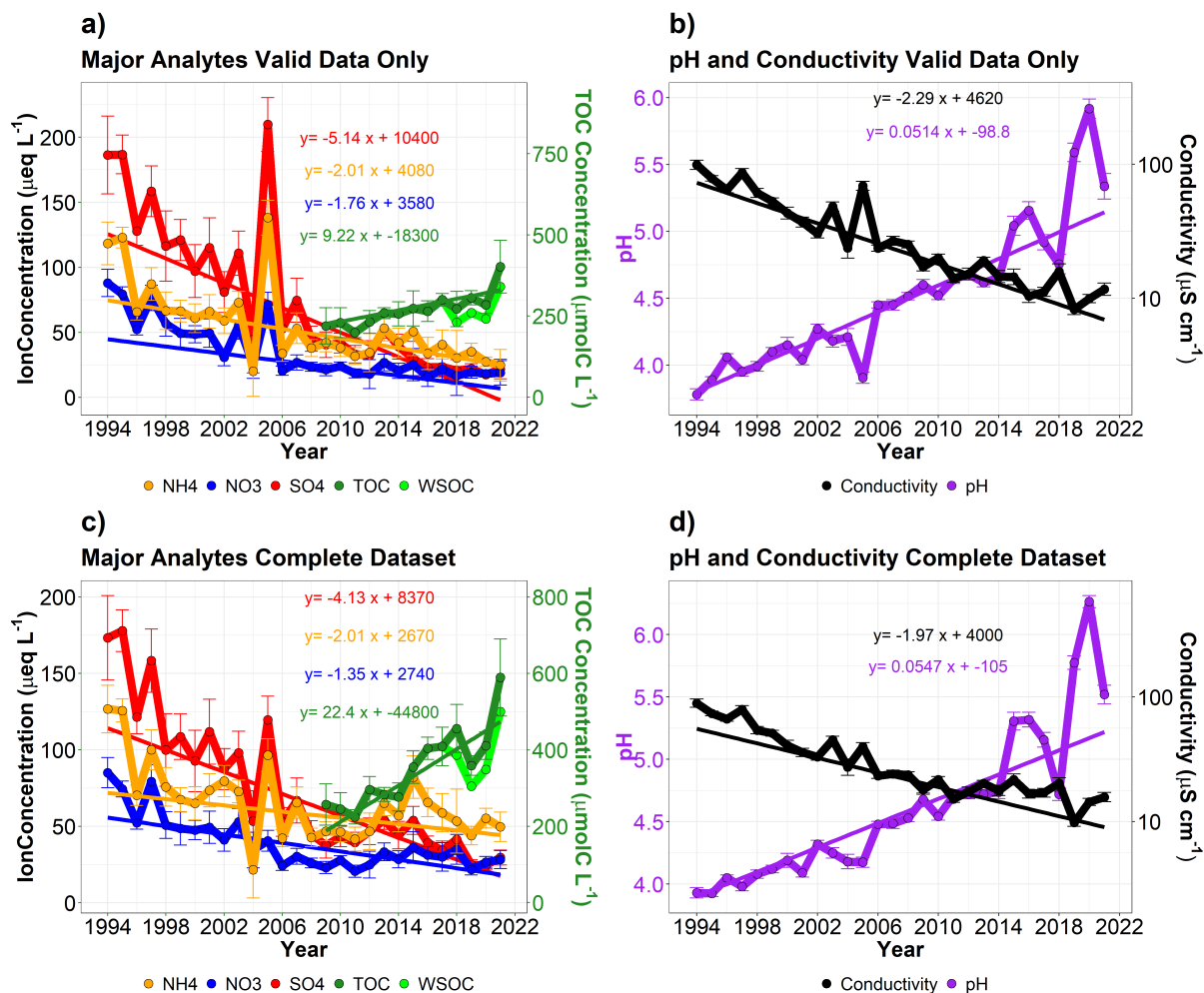


Figure 3. Annual median trends in cloud water collected from the summit of WFM. Plots a and b include Valid data, samples achieving an approximate ion balance, while plots c and d include the entire available dataset. Annual median trends in major analyte concentrations reported in $\mu\text{eq L}^{-1}$ for ions on the left axis, and $\mu\text{mol C L}^{-1}$ for TOC on the right axis. Conductivity is measured in $\mu\text{S cm}^{-1}$ on the right axis in plots b and d. Measured annual median WSOC for samples collected in 2018–2021 are shown in light green for comparison to the estimated TOC concentrations in these years. Error bars represent mean standard error.

analysis, as the median is more robust to outliers and a better representation of the population. Additionally, due to significant variance within the trend data, Mann-Kendall (MK) trend tests combined with Theil-Sen slope estimators (Sen, 1968) were employed to obtain a robust estimate of the slope of the long-term trends in measured analyte concentrations, with its



3 Long-Term Trends

3.1 Trends in Valid Data

This section updates the long-term trends in cloud water composition at WFM that were previously reported by Aleksic et al. (2009), Dukett et al. (2011) and Schwab et al. (2016b), now including data through 2021. Figure 3a) shows annual median
220 analyte concentrations, and the slopes of the linear trend analysis for the Valid dataset, while table S1 a) shows the slopes, and associated p-values for all measured analytes. Annual median cloud water pH increased from 3.78 in 1994 to 5.34 in 2021, corresponding with a substantial decrease in conductivity and SO_4^{2-} . Meanwhile, NO_3^- , NH_4^+ , and Cl^- concentrations exhibited relatively modest decreases, which leveled off starting in 2006. The remaining ions exhibited no discernible trends. TOC is the only analyte that shows evidence of an increasing trend (plotted on the right axis in the upper plot, Fig. 3a). This
225 is the first reported long-term trend for cloud water TOC at WFM. It should be noted that for 2009, the first year of routine TOC measurements, TOC analysis was only conducted on 20 samples in total, compared to 80-285 samples per year with TOC measurements from 2010-2021. In spite of the small samples size for 2009, these data are included in the trend analysis, as there is no evidence of measurement error or bias, and their inclusion doesn't strongly impact the resulting trend. Since TOC concentrations could not be measured for samples when automated filtering was performed during collection (as applied
230 for samples 2018-2021), annual median TOC concentrations for these 4 years were estimated based on the average 85% WSOC/TOC ratio observed for the subset of samples from 2018 and 2019 where both WSOC and TOC were measured (Fig. S1). Both WSOC and TOC concentrations are shown in Fig. 3a for these four years, but only the estimated TOC concentrations are used in the trend analysis.

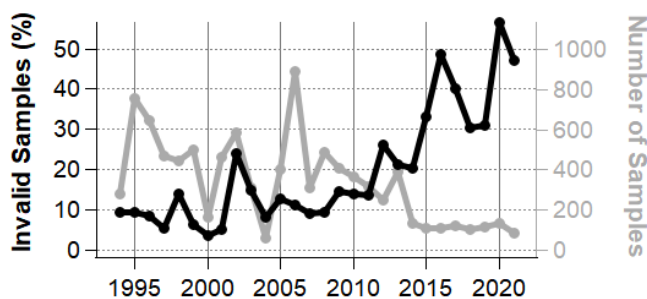


Figure 4. Annual percentage of cloud water samples considered Invalid according to ion balance criteria [Invalid/(Invalid + Valid)] (black, left axis) and total number of samples (Valid + Invalid + Unclassified) in each year (grey, right axis).

3.2 The Growing Influence of Invalid Data

235 Review of the cloud water measurements obtained at WFM shows that the proportion of so-called Invalid samples has increased substantially over the past several years, increasing from 9.3% in 1994 to 47% in 2021, and peaking at 57% in 2020 (Fig. 4).



This classification, based on ion balance criteria, was intended to reduce the impact from measurement error, as it is assumed that positively charged cations should be balanced by negatively charged anions in any natural bulk water systems. Implicit in this characterization is the assumption that the majority of ions are being measured. This growing ion imbalance in cloud water coincides with increasing cation/anion ratio observed in rain water collected by the National Atmospheric Deposition Program (NADP) over the same time period throughout NY State using the same standard suite of analytes (Rattigan et al., 2017). Since the rain water observations are entirely independent of the cloud water measurements, it is unlikely that the growing number of Invalid samples is due to a measurement artifact. Crucially, aside from ion imbalance, there is no evidence that the so-called Invalid cloud water samples were subject to measurement bias and should be discarded. We hypothesize, instead, that the growing ion imbalance is due to unmeasured ions, such as organic acids (Dukett et al., 2011), that are growing in abundance. Since organic acids are known to comprise a significant fraction of TOC (Herckes et al., 2013), the measured trend in TOC concentrations at WFM supports this hypothesis.

Since the Invalid data set now comprises nearly half of the samples it is worth analyzing this dataset separately. These samples are potentially representing a chemically distinct subset of samples that are encountered more frequently in recent years. To summarize, Invalid samples are considerably less acidic (0.5-1 pH units) and exhibit higher concentrations of NH_4^+ , TOC, Ca^{2+} and K^+ (Fig. S3), and the trends are significantly different as well. After around 2006, trends in the Invalid dataset appear to begin diverging from the Valid data set. On average, LWC is higher within the Valid data set, which tends to dilute samples and thus reduce all analyte concentrations. However, there is not a growing divergence between the trends of Valid and Invalid LWC, therefore LWC trends alone do not explain the divergence between Valid and Invalid concentrations. These observations show that while the Invalid samples have been growing more common, the composition of the Invalid samples has also grown more concentrated in TOC, NH_4^+ , NO_3^- and Ca^{2+} over the past decade.

3.3 Trends of the Complete Data Set

Including Valid, Invalid and unclassified data, the trends still exhibit significant reductions in conductivity, SO_4^{2-} , NO_3^- and NH_4^+ concentrations (Figure 3b and Table 1b). However the reductions are lower in magnitude compared to only the Valid data. For instance, the slope of the regression line of $[\text{SO}_4^{2-}]$ decreases from 5.14 to 4.13 $\mu\text{eq L}^{-1} \text{yr}^{-1}$. Notably, the reactive nitrogen species (NH_4^+ and NO_3^-) exhibit a more noticeable uptick in recent years from the overall downward linear trend. This apparent inflection point in the trends starting around 2006 appears to signify the emergence of a new chemical regime that has been growing in importance with the growing fraction of Invalid samples. The biggest impact of including the Invalid data in our analysis is a stronger increasing trend in TOC concentrations, which more than doubles from 2009 to 2021. $[\text{Ca}^{2+}]$ and $[\text{Mg}^{2+}]$ also show strong increasing trends. Annual median concentrations for the complete dataset show that NH_4^+ has been increasingly capable of neutralizing SO_4^{2-} and NO_3^- , which is well matched by a decreasing trend in measured H^+ (Fig. 5). Note that for individual cloud water samples, $[\text{NH}_4^+]$ can be greater than both $[\text{SO}_4^{2-}]$ and $[\text{NO}_3^-]$ combined, which occurred for 1203 out of 9429 cloud water samples from 1994 to 2021.

The increasing trend in annual median Cation/Anion ratios within cloud water over the entire record is 1.97% yr^{-1} ($p < 0.001$), including only samples where cations and anions for all measured analytes are reported. Emergence of a new chemical

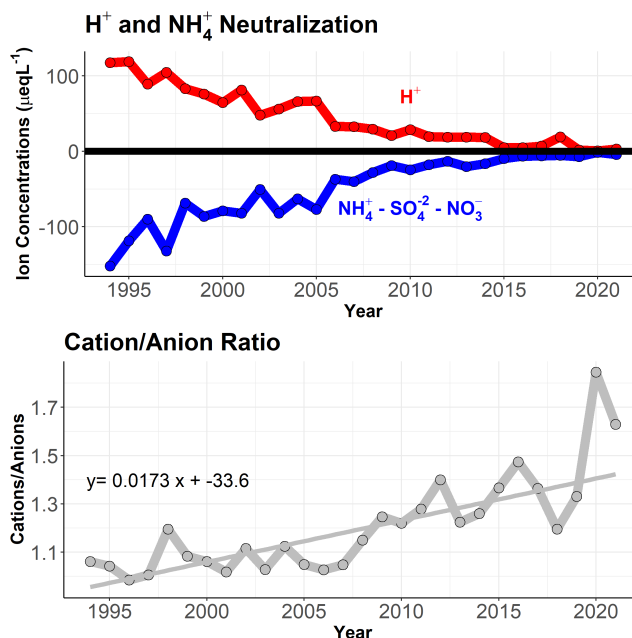


Figure 5. a) Annual median measured H⁺ concentrations and neutralization of SO₄²⁻ and NO₃⁻ by NH₄⁺, and b) annual median Cation/Anion ratios, in cloud water collected from the summit of WFM (complete dataset).

regime within the past decade is further supported by these observations, with annual median ion imbalance < 20% prior to 2009, after which median ion imbalance has exceeded 20% in every subsequent year except 2018.

4 Relationship Between Cloud Chemistry and Liquid Water Content

The analysis so far has focused on cloud water concentrations, which can be impacted by changes in meteorological parameters like LWC that are unrelated to changes in chemistry or emissions. Previous works have investigated the role of LWC on analyte concentrations (Elbert et al., 2000; Aleksic and Dukett, 2010; van Pinxteren et al., 2016), finding a weak non-linear negative relationship between total ion concentrations (TIC) and LWC, with considerable variance within the data. Aleksic and Dukett (2010) used a probabilistic technique to describe the relationship between binned LWC and TIC, with TIC showing a negative exponential relationship with LWC. When using this type of LWC binning technique for TOC, a similar probabilistic relationship can be found (Fig. S4), where a decreasing trend is observed in TOC as LWC increases, but exhibiting large variability within each bin, similar to what has been found previously at other locations (Herckes et al., 2013).

An alternate way to report cloud and precipitation composition is to weight by sample volume (Schwab et al., 2016a; Rattigan et al., 2017), which provides a means for determining the net accumulation of a particular analyte in the environment. Sample volume for cloud water is dependent on the collection efficiency of the cloud water collector, which is influenced by wind speed, LWC and updraft, complicating the relationship between sample volume and cloud composition. In our analysis,

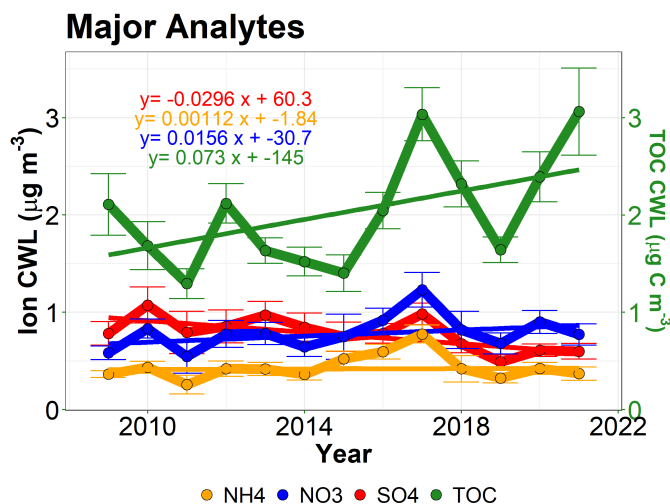


Figure 6. Linear trends in annual median Cloud Water Loadings (CWL) between 2009–2021 for the complete data set, using the meteorology criteria outlined in the SI, Section 1 to calculate average in-cloud LWC values associated with each sample.

instead of sample volume, samples are weighted by liquid water content (LWC) to determine Cloud Water Loadings (CWL), also referred to as air-equivalent concentrations (Marinoni et al., 2004; Wang et al., 2016; Kim et al., 2019), which has the added advantage of being directly comparable to aerosol loadings.

Figure 6 and Table S2 show the trends and the associated p-values in median CWL for 2009–2021, a time period for which meteorological data was available for calculating the average in-cloud LWC for each cloud water sample within the complete dataset. Focusing on this date range has the added advantage of focusing on a time period that is chemically distinct from the earlier half of the long-term record (e.g. with NH₄⁺ concentrations growing in abundance relative to both SO₄²⁻ and NO₃⁻, and changing trends in all the major analytes, as shown in Fig. 3c). Using the same analysis method as in previous sections, increasing trends in Ca²⁺, Mg²⁺, Na⁺, Cl⁻, and K⁺ CWL since 2009 are observed. The trends in Ca²⁺ and Mg²⁺ CWL imply increased influence from mineral or soil dust, while the increasing trends in Na⁺ and Cl⁻ suggest increasing influence from sea spray or playa dust. The increasing K⁺ trend could indicate increased influence from wildfires (Simoneit, 2002; Pachon et al., 2013), though K⁺ can also be found in coarse mode aerosol (VandenBoer et al., 2011). Meanwhile, there is no statistically significant trend in LWC, SO₄²⁻, NH₄⁺, NO₃⁻ or TOC CWL over this time period. This surprising result indicates that the large increasing trend in TOC concentrations since 2009 reported in Fig. 3c is not statistically significant when accounting for LWC, despite the positive slope of the TOC CWL regression line. Additional measurement uncertainty introduced by the LWC measurements may partly account for the higher p-value and reduced significance of the TOC CWL trend, but complex relationships between LWC and TOC concentrations (e.g. dilution and partitioning of soluble organic gases and/or drier air masses associated with greater biomass burning emissions) could all be playing a role.



5 Potential Missing Ions

305 Two independent measures (Cation/Anion ratio and Predicted/Measured Conductivity) imply that as pH increases, there is a growing abundance of analytes that are not being measured, particularly above 4.5 pH (Fig. S5). The measured ion imbalance suggests that more of the missing analytes are anions than cations. Here, we discuss potential missing anions responsible for the increasing trend in cation/anion ratios in WFM cloud water.

5.1 Bicarbonate

310 Due to increasing cloud water pH, bicarbonate (HCO_3^-) is hypothesized to have a growing contribution to ion balance. The dissolution of CO_2 is a major source of HCO_3^- by partitioning into cloud droplets and hydrolyzing to form carbonic acid (H_2CO_3). This contribution of HCO_3^- from CO_2 increases as pH increases. Highly alkaline dust particles containing calcium and magnesium carbonate (CaCO_3 and MgCO_3) can also be a major source of HCO_3^- . Cloud water collection sites that are heavily influenced by mineral dust often report pH values above 7 (Khemani et al., 1987; Budhavant et al., 2014), leading
315 to relatively acid-buffered cloud water. While the suite of measurements at WFM did not include HCO_3^- , it can be estimated using pH dependent equilibrium equations for an aqueous system open to the atmosphere, calculated as follows:

$$[\text{HCO}_3^-] = \frac{P_{\text{CO}_2} * H_{\text{CO}_2} * K_{a1}}{[\text{H}^+]} \quad (3)$$

where P_{CO_2} represent the partial pressure of CO_2 , assumed to be 410 ppm, $H_{\text{CO}_2} = 3.2 \times 10^{-2} \text{ M atm}^{-1}$ is the Henry's law constant of CO_2 and $K_{a1} = 4.37 \times 10^{-7}$ (Sander, 2015). Temperature was also assumed to be 298 K. There is virtually
320 no change to the overall ion balance when including estimated HCO_3^- (Fig. S6). Even for pH values above 6 (approximately the $\text{p}K_a$ of H_2CO_3), there are only modest improvements in overall ion balance. Based on these estimates, it is unlikely that HCO_3^- is a major driver of ion imbalance in the WFM cloud water observations. Importantly, these are only estimates of $[\text{HCO}_3^-]$ based on equilibrium with the atmosphere. There has been significant discussion on the validity of Henry's Law constants for cloud drop distributions, as several field studies note significant departures of measurements from gas-aqueous
325 phase partitioning (Pandis and Seinfeld, 1991; Winiwarter et al., 1994; Straub, 2017). It is plausible that some deviations could also exist for the carbonate system, thus leading to inaccurate HCO_3^- concentration estimates. One fog water monitoring site in Pennsylvania found similar anion deficiency in their system and hypothesized HCO_3^- as one potentially missing anion. For better estimates, they used inorganic carbon measurements from a TOC analyzer and assumed all inorganic carbon was part of the carbonate system. They then used the pH of the fog water to calculate the fraction of HCO_3^- . This led to around a 2.4x
330 greater concentrations of HCO_3^- on average than predictions based on Henry's Law, improving overall ion balance (Straub, 2017). It should be noted that the fog water exhibited considerably greater pH values than WFM cloud water, however, and only fog water samples with $\text{pH} > 6.0$ showed appreciable ion imbalance, reinforcing our assessment that $[\text{HCO}_3^-]$ are likely negligible for the majority of cloud water samples from WFM.



5.2 Organic Anions

335 Organic anions such as formate, acetate, and oxalate are known to be present in cloud and rain water, including at WFM
(Khwaja et al., 1995; Chapman et al., 2008; Herckes et al., 2013; Akpo et al., 2015). A strong correlation between TOC and
ion imbalance ($R^2 = 0.55$, $p < 0.001$), implies that an important fraction of missing anions are likely organic (Fig. S7). Further
evidence for missing organic acids is revealed when investigating ion balance as a function of pH. At low pH, the ratio of
measured Cations to Anions is approximately 1, approaching ion balance. As pH increases, the ratio decreases, reaching a
340 minimum of 0.69 for pH 5.5-6.3, with large decreases in the ratio at pH bins of 4.0-4.8 and 4.8-5.5 (Fig. S8). These pH bins
are close to the pKa values of formic and acetic acid (3.74 and 4.75 respectively), often the most abundant organic acids
found in cloud water (Herckes et al., 2013). As pH increases, a greater fraction of these acids, and others, are expected to
exist in their anionic form, and contribute more significantly to charge balance. Similarly, Figure 5s shows that the ratio of
predicted/measured conductivity decreases as pH increase, indicating a missing source of ions within the system that could be
345 organic in nature. In order to better constrain the growing ion imbalance in cloud water at WFM, the concentration of organic
anions such as organic acids must be routinely measured and their protonation state determined.

6 A New Chemical Regime

6.1 Changing Relationship Between H^+ and Conductivity

While our analysis of the long-term cloud water data set at WFM illuminates important differences from previous analyses,
350 there is no doubt that significant progress has been made in reducing ambient concentrations of criteria pollutants across the
U.S. and at WFM since the 1990s, resulting in significant decreases in SO_4^{2-} and NO_3^- concentrations, with associated increases
in cloud water pH and decreases in conductivity. These overall trends highlight that, generally, conductivity is controlled by H^+
concentrations, due to the high limiting molar conductivity of H^+ ($\Lambda^+ = 349.5 \text{ S cm}^2 \text{ mol}^{-1}$) compared to other analytes (e.g.
160.0 $\text{S cm}^2 \text{ mol}^{-1}$ for SO_4^{2-} and 73.5 $\text{S cm}^2 \text{ mol}^{-1}$ for NH_4^+) (Coury, 1999). In recent years, this relationship is diminishing.
355 Figure 8a shows the relationship between conductivity and pH for individual cloud water samples throughout the entire 28 year
record (1994-2021). pH values range from <3 to nearly as high as 7, and conductivity values likewise span nearly 3 orders
of magnitude. Many samples exhibit a strong linear relationship between H^+ and conductivity, especially in more acidified
cloud samples. However, beginning at pH values above 4, many samples deviate from this linear relationship, with higher
conductivity values than expected for samples with high pH. To reach these same conductivity values, the cloud water samples
360 requires much higher concentrations of other ions such as NH_4^+ and Ca^{2+} . The emergence of this new 'Non-Linear Regime'
with both high pH and high conductivity implies that one cannot assume that samples with higher pH are 'cleaner', as was

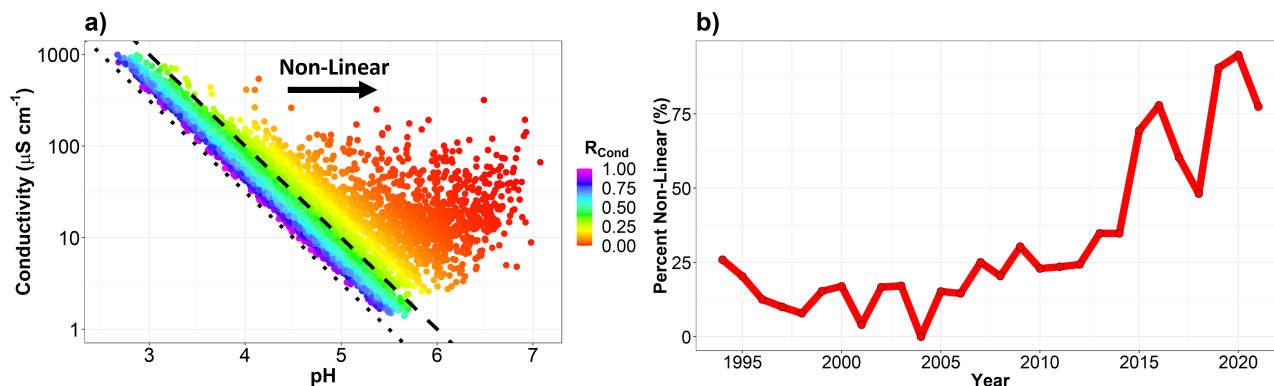


Figure 7. a) Conductivity and pH for individual cloud water samples from 1994 to 2021. The Linear and Non-Linear regimes are distinguished with dashed line that indicates H^+ contribution to the measured conductivity is exactly 35%. To the right of this line, H^+ contributes less to the measured conductivity, and we refer to this as the Non-Linear Regime, since conductivity and pH no longer exhibit a clear linear relationship. The dotted line represents the conductivity if H^+ is the only ion present. b) Percent of samples in the Non-Linear Regime for each year of sampling at WFM.

typically the case in decades past at WFM. To better investigate this non-linear relationship between conductivity and H^+ , we propose a new method of classifying cloud water data as follows:

$$R_{\text{Cond}} = \frac{H_{\text{Cond}}}{M_{\text{Cond}}} \quad (4)$$

365 where M_{Cond} is the measured specific conductivity and H_{Cond} is the conductivity from the H^+ ion, calculated from:

$$H_{\text{Cond}} = \Lambda^+ [H^+] \quad (5)$$

where Λ^+ is the limiting molar conductivity of the H^+ ion at infinite dilution arising from the autoionisation of pure water. If $R_{\text{Cond}} < 0.35$, less than 35% of the total conductivity of the sample can be explained by H^+ . For samples with $R_{\text{Cond}} > 0.35$, to the left of the dashed line on Fig. 7a, a linear relationship between conductivity and pH is observed, and for samples with
 370 $R_{\text{Cond}} < 0.35$ this linear relationship breaks down. The following section will compare differences in chemistry between the two regimes.

6.2 Linear Regime vs Non-Linear Regime

There are many similarities between the Valid/Invalid and Linear/Non-Linear classifications. Figure 7b shows that a growing fraction of samples are in the Non-Linear Regime, peaking at over 90% of samples in 2020. Table 1 uses a Dunn test to compare
 375 median concentrations between the Linear and Non-Linear regimes (averaged over all years for which data is available, i.e. 1994-2021 for all analytes except for TOC, which was averaged over 2009-2021). Conductivity and SO_4^{2-} are nearly double



Dunn-Test Comparison of Regimes

Species	Non-Linear Median	Linear Median	Difference	Percent Difference	p-value	Non-Linear n	Linear n
TOC (umolC/L)	424.641	236.067	188.574	44.408%	p < 0.001	745	836
NH4 (ueq/L)	77.767	55.513	22.255	28.616%	p < 0.001	1873	6357
SO4 (ueq/L)	42.890	86.653	-43.763	-102.035%	p < 0.001	1863	6377
Ion Balance (ueq/L)	37.514	6.999	30.515	81.343%	p < 0.001	1823	6172
NO3 (ueq/L)	33.310	36.382	-3.072	-9.222%	0.823	1874	6377
Ca (ueq/L)	28.202	5.725	22.477	79.700%	p < 0.001	1866	6350
Conductivity (uS/cm)	21.210	40.600	-19.390	-91.419%	p < 0.001	1879	6431
Mg (ueq/L)	6.144	1.811	4.333	70.524%	p < 0.001	1865	6329
pH	5.285	4.190	1.095	20.719%	p < 0.001	1879	6431
Cl (ueq/L)	2.962	2.426	0.536	18.096%	p < 0.001	1862	6354
Na (ueq/L)	1.740	0.968	0.772	44.368%	p < 0.001	1852	6342
K (ueq/L)	1.540	0.928	0.612	39.740%	p < 0.001	1853	6291
LWC (g/m ³)	0.425	0.570	-0.145	-34.118%	p < 0.001	1811	5976

Table 1. Linear versus Non-Linear Regime median concentrations for all measured analytes and associated p-values for the Dunn test.

and cloud water pH is 1 unit lower in the Linear data set compared to the Non-Linear data set, highlighting the dominance of SO_4^{2-} and H^+ in the Linear Regime. There is no obvious difference in NO_3^- concentrations between the two data sets, implying that the controlling factors for NO_3^- are unrelated to the relationship between H^+ and conductivity. Every other measured ion shows higher concentrations in the Non-Linear data set than the Linear data set, with considerably higher concentrations of TOC, Ca^{2+} , and Mg^{2+} , and in addition, an overall greater ion imbalance. Therefore, the Linear Regime can be characterized as a highly acidified system controlled by SO_4^{2-} , and the Non-Linear Regime is a system with greater TOC, NH_4^+ and base cations. The Non-Linear Regime is becoming the predominate system in WFM cloud water.

6.3 Is Cloud Water Representative of Cloud Droplets?

With the reductions in SO_4^{2-} and NO_3^- , species such as Ca^{2+} have grown in relative importance to ion balance, conductivity, and pH. Sources of atmospheric Ca^{2+} can include fossil fuel combustion in the form of fly ash (Lee and Pacyna, 1999), but the major source is generally thought to be mineral dust particles containing bases like calcium carbonate (CaCO_3) and calcium oxide (CaO). These particles typically raise the pH of cloud and rain water, particularly evident in observations reported from measurements in India (Khemani et al., 1987; Budhavant et al., 2014). Within WFM cloud water, there is a considerably higher concentration of Ca^{2+} for samples within the Non-Linear Regime, likely contributing, in part, to the higher measured pH values.

Due to the mechanism by which they are lofted into the atmosphere, mineral dust aerosols are known to exist primarily in the coarse mode (i.e., with dry particle diameter > $1\mu\text{m}$) (Seinfeld and Pandis, 2016). While these aerosol can make up a substantial fraction of the overall aerosol mass concentration, they generally represent a very small fraction of the aerosol number concentration (Mahowald et al., 2014). Therefore, even if these particles are hygroscopic, only a small fraction of activated



cloud droplets are likely affected by coarse mode aerosol, even at a remote location like WFM where aerosol concentrations are relatively low. During a pilot study at WFM in 2017, cloud droplets intercepted at the summit of WFM were shown to be primarily comprised of cloud condensation nuclei with 100-300nm dry diameter (Lance et al., 2020), consistent with this general understanding.

400 When the rare alkaline cloud droplets, formed on coarse mineral dust aerosol, are collected by the cloud water collection system, they can have an out-sized impact on the bulk cloud water sample, which may no longer well represent the majority of cloud droplets as they existed in the cloud. This is supported by work from Moore et al. (2004) using a multistage cloud collector at WFM, which found that Ca^{2+} and Mg^{2+} concentrations were 1.9-30 and 2.3-58 times greater, respectively, in large droplets than small droplets. Size resolved aerosol composition data in nearby Ontario, Canada indicates that 65-95%
405 of the total aerosol Ca^{2+} mass and 78-99% of Mg^{2+} were within super micron ($> 1 \mu\text{m}$) aerosol in 2009-2010 when those measurements were conducted (VandenBoer et al., 2011). However, $> 99\%$ of the total number of aerosol were found in sub micron particles. A wide range (11-71%) of K^+ was found to reside in super micron aerosol, suggesting that while a significant fraction of K^+ can be associated with mineral dust, an important fraction can also come from non-dust sources like biomass burning. The fraction of NO_3^- within coarse mode aerosol was also found to be highly variable, ranging from 21-93%. While
410 NO_3^- often resides with fine mode aerosol, gaseous HNO_3 can react with coarse mode aerosol containing alkaline species like CaCO_3 and MgCO_3 (Hansen et al., 2010; Hrdina et al., 2021) resulting in coarse mode aerosol NO_3^- (Fig. S9).

Based on this general understanding of coarse mode aerosol, as discussed above, we expect that bulk collection of cloud water is often no longer representative of the vast majority of cloud droplets as they existed in the atmosphere and could bias our understanding of cloud droplet pH. In an attempt to better account for this potential bias, a new calculation for inferred pH
415 of a typical cloud droplet (pH_{TD}) is introduced:

$$\text{pH}_{\text{TD}} = -\log_{10}([\text{H}^+] + [\text{Ca}^{2+}] + [\text{Mg}^{2+}]) \quad (6)$$

where $[\text{H}^+]$, $[\text{Ca}^{2+}]$ and $[\text{Mg}^{2+}]$ are the measured concentrations in units of eq L^{-1} within bulk cloud water. We refer to this as the "top down" (TD) approach for estimating acidity of the majority of cloud droplets because the measured bulk cloud water pH provides the cumulative impact from all dissolved molecules. By accounting for measured Ca^{2+} and Mg^{2+} concentrations,
420 this calculation is an attempt to remove the influence of mineral dust particles on the bulk cloud water pH. This calculation assumes that measured Ca^{2+} and Mg^{2+} ions are associated with dissolved alkaline compounds such as CaCO_3 or MgCO_3 in equilibrium with atmospheric CO_2 and that a very small number of droplets contain these minerals at all, as supported by the size-resolved aerosol composition measurements described above. While the measured pH of bulk cloud water is relevant for wet deposition, we posit that pH_{TD} is more relevant for processes occurring within the majority of cloud droplets as they
425 existed in the atmosphere.

We also calculate one of the simplest proxies for pH that has long been used to estimate fine mode aerosol pH (Pye et al., 2020):

$$\text{pH}_{\text{BU}} = -\log_{10}([\text{SO}_4^{2-}] + [\text{NO}_3^-] - [\text{NH}_4^+]) \quad (7)$$

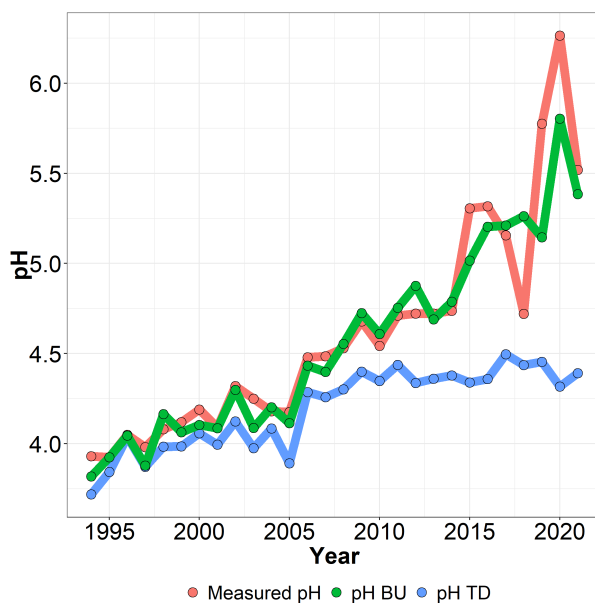


Figure 8. Annual median bulk cloud water pH (red) compared to estimated cloud droplet pH calculated from the bulk cloud water pH and measured Ca^{2+} and Mg^{2+} concentrations (pH_{TD} , blue) and estimated cloud droplet pH calculated from measured SO_4^{2-} , NO_3^- and NH_4^+ concentrations (pH_{BU} , green).

This "bottom up" (BU) proxy includes the major inorganic species typically found within fine mode aerosol, which are thus expected to be found in the majority of cloud droplets. Measured bulk NO_3^- concentrations are assumed to reside exclusively within the fine mode aerosol. Additional NH_3 or HNO_3 partitioning to cloud droplets subsequent to activation are also accounted for with this method, assuming partitioning to droplets formed on coarse mode aerosol is negligible. However, contributions from organic acids present in aerosols or partitioning to the aqueous phase during cloud droplet activation are entirely neglected.

Figure 8 shows the annual median trends of inferred cloud droplet pH (pH_{TD}) and measured bulk cloud water pH. During the first ~ 15 years of the cloud water monitoring program, pH_{TD} tracks closely with pH_{meas} , but the influence of base cations on measured pH has grown over time. Despite measured pH continuing to increase after 2010, there has been little change in pH_{TD} . In 2020, mineral dust is estimated to have increased the median cloud droplet pH from 4.5 to 6.3, resulting in more than an order of magnitude decrease in median H^+ concentrations.

Throughout the cloud water monitoring program, annual median pH_{BU} tracked measured bulk cloud water pH surprisingly well. This makes sense during the early years of the program when SO_4^{2-} , NO_3^- and NH_4^+ dominated the cloud water ionic composition and Ca^{2+} and Mg^{2+} had minimal impact on bulk cloud water acidity. However, the apparent agreement between pH_{BU} and pH_{meas} in recent years may be misleading. It should be noted that a substantial fraction of cloud water samples



exhibit greater NH_4^+ than $\text{SO}_4^{2-} + \text{NO}_3^-$ in recent years, corresponding to negative values for $[\text{H}^+]_{\text{BU}}$. This is a significant
445 limitation for this proxy method in recent years, when nearly 50% of cloud water samples exhibit this condition (Fig. 9a).

The large and growing discrepancy between bulk cloud water pH and pH_{TD} over the past decade coincides with the growing
fraction of samples being characterized in the Non-Linear Regime. We posit that, with SO_4^{2-} concentrations decreasing at
the same time base cations and TOC concentrations increase, the major influences on cloud droplet pH are also changing.
When we segregate individual cloud water samples by the Linear and Non-Linear regimes (Fig. 9b and c, respectively), we
450 can more clearly see how the different pH proxies compare. Within the Linear Regime, $[\text{H}^+]_{\text{BU}}$ (plotted on the x-axis in
Fig. 9b and c) shows a strong correlation with measured bulk cloud water $[\text{H}^+]$ but overpredicts measured $[\text{H}^+]$ by 11%.
Removing the influence of coarse mode aerosols by including $[\text{Ca}^{2+}]$ and $[\text{Mg}^{2+}]$ in the $[\text{H}^+]_{\text{TD}}$ calculation improves the
agreement, with a nearly 1:1 relationship between $[\text{H}^+]_{\text{TD}}$ and $[\text{H}^+]_{\text{BU}}$. Within the Non-Linear Regime, $[\text{H}^+]_{\text{BU}}$ greatly
overpredicts measured bulk cloud water acidity. When removing the influence of coarse mode aerosol, the correlation improves
455 but $[\text{H}^+]_{\text{BU}}$ underpredicts $[\text{H}^+]_{\text{TD}}$ by 14%. It's important to note that Fig. 9b and c only include samples where $[\text{SO}_4^{2-}] + [\text{NO}_3^-]$
> $[\text{NH}_4^+]$, which removes a growing fraction of samples from the analysis, potentially underestimating the fraction of acidity
from unmeasured ions in the system. Additionally, a Theil-Sen Regression was used to provide a robust estimate of the slope
between $[\text{H}^+]_{\text{BU}}$ and measured bulk cloud water $[\text{H}^+]$ and $[\text{H}^+]_{\text{TD}}$. This method was used as there were a few outlier samples
that were having an outsized impact on the regression line when using ordinary least squares regression, particularly within the
460 Non-Linear regime.

It is also important to note that even though pH shifts when accounting for the influence from rare alkaline droplets, the
cation/anion ratio for cloud droplets remains exactly the same as it was for bulk cloud water since the increased H^+ is exactly
balanced by the removal of the two base cation species (Ca^{2+} and Mg^{2+}), so the reassessment of bulk cloud water data in
terms of inferred cloud droplet acidity does not resolve the ion imbalance problem. This may point to a more important role
465 for organic acids in ion balance and acidity, which is a significant departure from the original intent of the collection site to
monitor and investigate largely inorganic acid deposition.

The top down and bottom up approaches described above provide two independent estimates for cloud droplet pH. By
comparing these two proxies, we then infer the percent of cloud droplet acidity that is unexplained by the major inorganic ions.
We define the Missing Acid Fraction (MAF) as:

470
$$\text{MAF} = \frac{[\text{H}^+]_{\text{TD}} - [\text{H}^+]_{\text{BU}}}{[\text{H}^+]_{\text{TD}}} \quad (8)$$

When MAF is zero, the measured SO_4^{2-} , NO_3^- and NH_4^+ concentrations are sufficient to explain 100% of the inferred cloud
droplet acidity, and when MAF is 1.0, the measured SO_4^{2-} , NO_3^- and NH_4^+ concentrations explain 0% of the inferred cloud
droplet acidity. In order to include cloud water samples where $[\text{NH}_4^+] > [\text{SO}_4^{2-}] + [\text{NO}_3^-]$ in this calculation, $[\text{H}^+]_{\text{BU}}$ was set
to zero for these samples, as SO_4^{2-} and NO_3^- are completely neutralized by NH_4^+ under these conditions and therefore do not
475 contribute to cloud water acidity. Fig. 10 shows the annual median MAF. Prior to ~ 2010 , $[\text{SO}_4^{2-}] + [\text{NO}_3^-] - [\text{NH}_4^+]$ explained the
majority of inferred cloud droplet acidity. Unmeasured ions may have contributed up to a quarter of cloud droplet acidity for

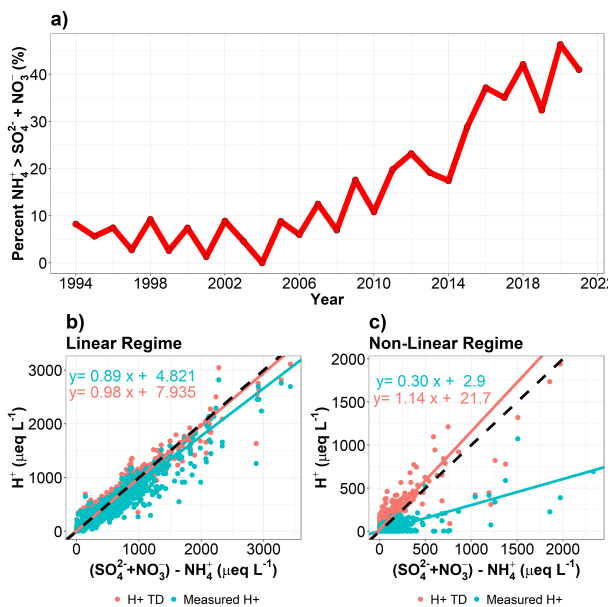


Figure 9. a) Percent of cloud water samples where NH_4^+ exhibits greater concentrations than $\text{SO}_4^{2-} + \text{NO}_3^-$ concentrations. Measured $[\text{H}^+]$ and inferred cloud droplet $[\text{H}^+]$ versus $[\text{SO}_4^{2-}] + [\text{NO}_3^-] - [\text{NH}_4^+]$ for the Linear and Non-Linear regimes, respectively, in b) and c). Slopes of the regression lines are calculated using a Theil-Sen regression. The dashed line represents a 1:1 line, when $[\text{SO}_4^{2-}] + [\text{NO}_3^-] - [\text{NH}_4^+]$ perfectly predicts H^+ .

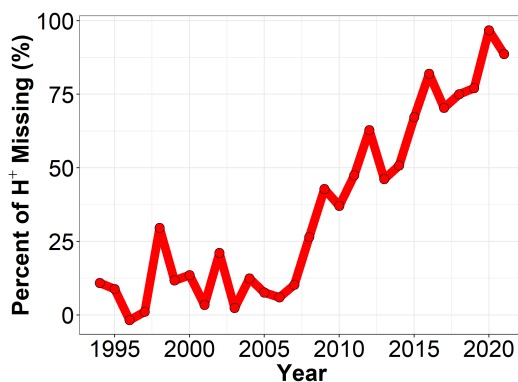


Figure 10. Annual median MAF throughout the long-term cloud water monitoring program, representing the fraction of inferred cloud droplet acidity that is not accounted for by the measured SO_4^{2-} , NO_3^- and NH_4^+ concentrations.

individual years during this time period, but the situation changed drastically in the following decade. A steady increase in the contribution of unmeasured ions to cloud droplet acidity over time is inferred since 2008, with the median MAF reaching nearly 100% in 2020. These trends signal a major shift of acidity being controlled predominantly by inorganic ions to potentially organic ions, a dramatic change from the concerns of acid deposition of the 1980s and 1990s.



There are a number of assumptions that must be recognized when interpreting results from this simple analysis. For a more precise estimate of typical cloud droplet acidity, other ions associated with coarse mode aerosol, like NO_3^- , would also be included in the pH_{TD} calculation. However, given that NO_3^- may be found predominantly in the coarse or fine mode at different times, the contribution from coarse mode NO_3^- is not sufficiently constrained by the measurements available. To
485 the degree that NO_3^- is present in coarse mode aerosol, Ca^{2+} and Mg^{2+} are expected to have less impact on cloud water alkalinity. By not factoring in the influence from coarse mode NO_3^- , pH_{TD} is likely a lower bound estimate for cloud droplet pH. Similarly, pH_{BU} would be underestimated to the same degree and for the same reason. A combination of NO_x reductions and potentially increasing dust aerosol within the region may be changing the fraction of NO_3 within fine mode aerosol, which would need to be better constrained to improve our pH_{BU} and MAF estimates. Also implicitly assumed is that LWC
490 associated with coarse mode aerosol is negligible for both the pH_{TD} and pH_{BU} proxies of cloud droplet pH. While the coarse mode aerosol can contribute significant aerosol mass in spite of low number concentrations due to their much larger size (1-2 orders of magnitude larger diameter for the coarse mode than the accumulation mode), the relative contribution of liquid water from cloud droplets formed on coarse mode aerosol is expected to be much lower due to the inverse relationship between condensational growth rate and droplet diameter, yielding droplets originating from the coarse and accumulation modes with
495 diameters within a factor of two of each other, for non-precipitating clouds (Seinfeld and Pandis, 2016).

Conversely, not accounting for the impact of size resolved aerosol composition on bulk cloud water pH may have a substantial impact on studies of gas/droplet/aerosol partitioning and aqueous chemistry (Pye et al., 2020). Size-resolved measurements of cloud droplet pH or Ca^{2+} and Mg^{2+} in aerosol and/or cloud droplets are required to confirm the validity of the pH_{TD} estimates reported here in order to confidently and accurately evaluate these types of atmospheric processes.

500 While the validity of the simple calculation for pH_{TD} cannot be directly evaluated with the current suite of measurements, it is encouraging that several important relationships are substantially simplified when evaluated against inferred cloud droplet pH instead of the measured pH. In particular, the relationship between pH_{TD} , LWC and SO_4^{2-} concentrations is much simpler and easier to explain, shown in Figure S11. For a given LWC, there is clearly an inverse relationship between SO_4^{2-} and pH_{TD} , which maxes out at $\text{pH}_{\text{TD}} \sim 5.6$ at the lowest SO_4^{2-} concentrations, coinciding with the pH expected for a pure water droplet in
505 equilibrium with atmospheric CO_2 . However, SO_4^{2-} concentrations exhibit a nonlinear relationship with measured pH values.

Another relationship that is simplified is the relationship between TOC concentrations and pH_{TD} . Figure 11 shows that TOC concentrations are much better correlated with pH_{TD} values throughout the entire data set (2009-2021), as compared to measured bulk cloud water pH. This might imply that, like SO_4^{2-} , organic compounds within cloud water are tightly linked with the cloud droplet pH. This finding may be consistent with the majority of organic aerosol mass being of secondary
510 origin (Jimenez et al., 2009), since several known mechanisms for secondary organic aerosol (SOA) formation include an acid catalyzed reaction step (Hallquist et al., 2009), and cloud droplet acidity is expected to correlate well with aerosol acidity for non-precipitating clouds. However, the other major secondary aerosol species (SO_4^{2-} , NH_4^+ and NO_3^-) also show simplified relationships with pH_{TD} as compared to measured bulk cloud water pH (Fig. S12). The simplified relationship between all of these analytes and pH_{TD} , may suggest that the formation mechanisms and/or emissions sources for these chemical species are
515 linked.

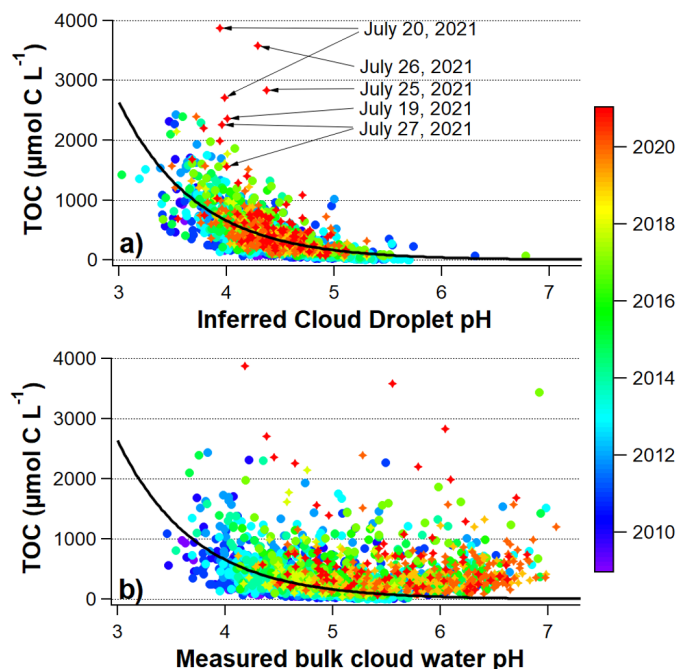


Figure 11. Measured TOC concentrations for individual samples 2009-2017 (circles) and measured WSOC concentrations for individual samples 2018-2021 (stars), versus a) inferred cloud droplet pH (pH_{TD}), and b) measured bulk cloud water pH, colored by the year that the cloud water sample was collected at WFM. The exponential curve in both a) and b) is the fit to all data in a): $\text{TOC}_{\text{fit}} = A \exp(-\text{pH}/\tau)$, $A = 1.7193 \times 10^5 \pm 2.6 \times 10^4$, $1/\tau = 1.3934 \pm 0.038$

Figure 11a highlights several cloud water samples with exceptionally high measured WSOC concentrations. While the majority of samples from 2018-2021 follow the long-term relationship between TOC and pH_{TD} , samples that don't follow this relationship have higher WSOC than any previously measured TOC concentrations throughout the long-term record. Two of the highest measured WSOC concentrations (2711 and $3878 \mu\text{mol C L}^{-1}$) occurred on July 19th and 20th, 2021, which
520 corresponded to a haze event across the northeastern U.S. associated with wildfire smoke originating mainly in central Canada (Popovich and Katz, 2021). Wildfire smoke can be an important source of both primary and secondary organic matter in both aerosol and cloud water, even significantly downwind (Cook et al., 2017; Di Lorenzo et al., 2018; Zhou et al., 2017). 5-day ensemble HYSPLIT back-trajectories launched on July 20, 2021 indicate the source location of the air mass originated from Eastern Manitoba, Canada, and Northeast North Dakota (Figure S12a). Black carbon and carbon monoxide measurements from
525 the summit of WFM on that day were also unusually high (e.g. as high as 1780 ng m^{-3} , compared to a more typical value of 100 ng m^{-3} black carbon). A WRF-Chem forecast shows elevated levels of CO attributed to wildfire smoke on July 15, 2021, with associated high levels of PM 2.5. Five days later, the WRF-Chem forecast shows similar elevated levels of wildfire CO and PM 2.5 over the Northeastern United States, further indicating an influence of Canadian wildfires impacting WFM (Figure S12b). More information about this WRF-Chem forecast can be found in Kumar et al. (2021). Several other samples with the



530 highest measured WSOC concentrations occurred that same week, as indicated in Fig. 11a. The relatively close proximity of these fires to WFM may be the reason for the exceptionally high WSOC concentrations and the strong deviation from the well established correlation with pH_{TD} . Episodic events with exceptionally high concentrations such as these are the reason we report annual median rather than annual mean concentrations for the long-term trends.

7 Summary and Conclusions

535 This work updates the long-term trend analysis of cloud water chemistry monitoring at Whiteface Mountain (WFM) over the past 28 years, with critical review of past methodologies resulting in significant changes to the data interpretation and additional analysis of TOC trends since 2009 when TOC was first routinely measured at WFM. In the past, many samples were excluded from analysis if they did not achieve an approximate ion balance from measured species. Using this criteria, a growing number of samples were being excluded from the data set, peaking at 57% of the samples, with no evidence of measurement error.

540 When evaluating the complete data set, decreases in SO_4^{2-} , NH_4^+ , and NO_3^- become more modest, TOC increases at a much faster rate, and increasing trends in Ca^{2+} and Mg^{2+} emerge. The increasing fraction of samples that do not achieve ion balance is associated with an increasing cation/anion ratio, implying there are anions that are not being measured and that are growing in abundance.

When evaluating changes in cloud water loading (CWL), the trend in TOC is no longer significant, indicating that much of

545 the trend in TOC was due to variability in LWC. There is also an increasing trend in trace ions like Ca^{2+} and K^+ .

When investigating potential missing anions, HCO_3^- and organic acids were identified as two important candidates. Estimates of HCO_3^- using cloud water pH, and atmospheric CO_2 indicate that for most cloud water samples, HCO_3^- is negligible. For samples with $\text{pH} > 6$, which are growing more common, HCO_3^- could be important. However, samples with bulk cloud water pH this high are often likely impacted by externally mixed alkaline droplets formed on coarse mineral dust aerosol that

550 don't represent the majority of cloud droplets as they existed in the atmosphere. Organic acids are therefore likely more important than HCO_3^- for explaining ion imbalance for the majority of cloud droplets originating from fine mode cloud condensation nuclei. VandenBoer et al. (2011) found that organic acids were found predominantly within submicron aerosol, which supports this hypothesis. The strong correlation between TOC and ion imbalance also supports this hypothesis, since organic acids are known to comprise a significant fraction of TOC.

555 In the early years of the cloud water monitoring program, conductivity was largely controlled by H^+ due to its high concentrations and large molar conductivity relative to other ions in the system. In recent years, conductivity is no longer linearly proportional to H^+ concentrations. We use the break down of the linear relationship between conductivity and H^+ to characterize a new chemical regime that is less acidic but exhibits high conductivity. A growing fraction of samples are now being classified in this Non-Linear Regime, peaking at over 90% of samples in 2020. The Non-Linear Regime is characterized by

560 higher concentrations of TOC, NH_4^+ , and base cations, particularly Ca^{2+} .

Altogether, the reduction of SO_4^{2-} and NO_3^- , and increases in Ca^{2+} and Mg^{2+} potentially bias the pH of bulk cloud water high, as these ions are expected to reside in coarse aerosol that only represent a small fraction of cloud droplets. To account



for this bias, we proposed a new calculation for “Inferred cloud droplet pH” that accounts for the measured Ca^{2+} and Mg^{2+} concentrations. While measured bulk cloud water pH has steadily increased for the entire duration of routine cloud water monitoring program, inferred cloud droplet pH has remained flat since 2009, implying that much of the increasing cloud water pH is driven by Ca^{2+} and Mg^{2+} rather than the reductions in SO_4^{2-} . In the Linear Regime, $\text{SO}_4^{2-} + \text{NO}_3^- - \text{NH}_4^+$ is a useful predictor for both measured bulk cloud water pH and inferred cloud droplet pH. In the Non-Linear Regime, the relationship with measured pH is very weak. The relationship improves when using inferred cloud droplet pH but significantly underpredicts measured cloud droplet pH. This analysis reveals a missing source of acidity that correlates with TOC, which needs to be accounted for as a majority of cloud water samples are now within the Non-Linear Regime. A growing number of samples exhibit NH_4^+ that is greater than the sum of SO_4^{2-} and NO_3^- , preventing the calculation of cloud droplet pH and providing further evidence of major missing source of acidity.

Considerable changes have occurred in cloud water at WFM over the past 28 years of monitoring, from a system dominated by SO_4^{2-} to a system more controlled by base cations and TOC. Many other regions in the world are seeing changes as SO_2 emissions continue to decrease. This type of system is considerably less studied, with important implications for air quality, ecosystem health, and climate. More research, in combination with additional measurements of aerosol and trace gases, are required to better understand the system. As WFM and potentially other regions of the world enter this new chemical regime, additional measurements will be needed to study the effect on important processes like secondary organic aerosol production, cloud processing and nitrogen deposition.

580 *Competing interests.* All authors declare no competing interests.

Code and data availability. Cloud water data can be found at <http://atmoschem.asrc.cestm.albany.edu/~cloudwater/pub/Data.htm>. The code and data used to make the figures can be found at <https://github.com/ChrisLaw08/LongTermTrendsProject>.

Author contributions. J. Dukett and P. Snyder conducted the cloud water sampling and chemical analysis 2001-2017. P. Casson, R. Brandt, C. Lawrence and S. Lance conducted the cloud water sampling 2018-2021. D. Kelting and L. Yerger conducted the chemical analysis 2018-2019. P. Snyder conducted the chemical analysis 2020-2021. C. Lawrence and S. Lance analyzed the data sets. C. Lawrence carried out the statistical analyses. C. Lawrence and S. Lance wrote the manuscript with contributions from all co-authors.

Acknowledgements. Cloud water measurements reported in this paper were supported by the New York State Energy Research and Development Authority (NYSERDA) under the Adirondack Long Term Monitoring project (2001-2017) and NYSERDA Contract 124461 (2018-2021). Previous cloud water measurements (1994-2000) conducted by MADPro were funded by the U.S. EPA under Contract 68-02-4451 and 68-D2-0134. WFM trace gas and meteorological measurements were supported by NYSERDA Contract 48971. NYSERDA has



not reviewed the information contained herein, and the opinions expressed in this report do not necessarily reflect those of NYSERDA or the State of New York. P. Casson and S. Lance thank Eric Hebert for helping to set up the cloud water collection system. S. Lance and C. Lawrence thank Gabriele Pfister and Rajesh Kumar of NCAR for providing output from the WRF-Chem forecast.



References

- 595 Akpo, A. B., Galy-Lacaux, C., Laouali, D., Delon, C., Liousse, C., Adon, M., Gardrat, E., Mariscal, A., and Darakpa, C.: Precipitation chemistry and wet deposition in a remote wet savanna site in West Africa: Djougou (Benin), *Atmospheric Environment*, 115, 110–123, <https://doi.org/10.1016/j.atmosenv.2015.04.064>, tex.ids= akpoPrecipitationChemistryWet2015a, akpoPrecipitationChemistryWet2015b, 2015.
- Aleksic, N. and Dukett, J. E.: Probabilistic relationship between liquid water content and ion concentrations in cloud water, *Atmospheric Research*, 98, 400–405, <https://doi.org/10.1016/j.atmosres.2010.08.003>, 2010.
- 600 Aleksic, N., Roy, K., Sistla, G., Dukett, J., Houck, N., and Casson, P.: Analysis of cloud and precipitation chemistry at Whiteface Mountain, NY, *Atmospheric Environment*, 43, 2709–2716, <https://doi.org/10.1016/j.atmosenv.2009.02.053>, 2009.
- Budhavant, K., Rao, P., Safai, P., Granat, L., and Rodhe, H.: Chemical composition of the inorganic fraction of cloud-water at a high altitude station in West India, *Atmospheric Environment*, 88, 59–65, <https://doi.org/10.1016/j.atmosenv.2014.01.039>, 2014.
- 605 Cape, J. N., Cornell, S. E., Jickells, T. D., and Nemitz, E.: Organic nitrogen in the atmosphere — Where does it come from? A review of sources and methods, *Atmospheric Research*, 102, 30–48, <https://doi.org/10.1016/j.atmosres.2011.07.009>, 2011.
- Chapman, P. J., Clark, J. M., Reynolds, B., and Adamson, J. K.: The influence of organic acids in relation to acid deposition in controlling the acidity of soil and stream waters on a seasonal basis, *Environmental Pollution*, 151, 110–120, <https://doi.org/10.1016/j.envpol.2007.03.001>, 2008.
- 610 Cook, R. D., Lin, Y.-H., Peng, Z., Boone, E., Chu, R. K., Dukett, J. E., Gunsch, M. J., Zhang, W., Tolic, N., Laskin, A., and Pratt, K. A.: Biogenic, urban, and wildfire influences on the molecular composition of dissolved organic compounds in cloud water, *Atmospheric Chemistry and Physics*, 17, 15 167–15 180, <https://doi.org/https://doi.org/10.5194/acp-17-15167-2017>, publisher: Copernicus GmbH, 2017.
- Coury, L.: *Conductance Measurements Part 1: Theory, Current Separations*, p. 6, 1999.
- Di Lorenzo, R. A., Place, B. K., VandenBoer, T. C., and Young, C. J.: Composition of Size-Resolved Aged Boreal Fire
615 Aerosols: Brown Carbon, Biomass Burning Tracers, and Reduced Nitrogen, *ACS Earth and Space Chemistry*, 2, 278–285, <https://doi.org/10.1021/acsearthspacechem.7b00137>, publisher: American Chemical Society, 2018.
- Driscoll, C. T., Driscoll, K. M., Fakhraei, H., and Civerolo, K.: Long-term temporal trends and spatial patterns in the acid-base chemistry of lakes in the Adirondack region of New York in response to decreases in acidic deposition, *Atmospheric Environment*, 146, 5–14, <https://doi.org/10.1016/j.atmosenv.2016.08.034>, 2016.
- 620 Dukett, J. E., Aleksic, N., Houck, N., Snyder, P., Casson, P., and Cantwell, M.: Progress toward clean cloud water at Whiteface Mountain New York, *Atmospheric Environment*, 45, 6669–6673, <https://doi.org/10.1016/j.atmosenv.2011.08.070>, tex.ids= dukettProgressCleanCloud2011, 2011.
- Elbert, W., Hoffmann, M. R., Krämer, M., Schmitt, G., and Andreae, M. O.: Control of solute concentrations in cloud and fog water by liquid water content, *Atmospheric Environment*, 34, 1109–1122, [https://doi.org/10.1016/S1352-2310\(99\)00351-9](https://doi.org/10.1016/S1352-2310(99)00351-9), 2000.
- 625 EPA: *Methods for Chemical Analysis of Water and Wastes.*, 1983.
- Falconer, R. E. and Falconer, P. D.: Determination of cloud water acidity at a mountain observatory in the Adirondack Mountains of New York State, *Journal of Geophysical Research: Oceans*, pp. 7465–7470, [https://doi.org/10.1029/JC085iC12p07465@10.1002/\(ISSN\)2169-9291.CACGP1](https://doi.org/10.1029/JC085iC12p07465@10.1002/(ISSN)2169-9291.CACGP1), publisher: John Wiley & Sons, Ltd, 1980.
- Gerber, H.: Direct measurement of suspended particulate volume concentration and far-infrared extinction coefficient with a laser-diffraction
630 instrument, *Applied Optics*, 30, 4824–4831, <https://doi.org/10.1364/AO.30.004824>, 1991.



- Gorham, E.: Acid deposition and its ecological effects: a brief history of research, *Environmental Science & Policy*, 1, 153–166, [https://doi.org/10.1016/S1462-9011\(98\)00025-2](https://doi.org/10.1016/S1462-9011(98)00025-2), tex.ids= gorhamAcidDepositionIts1998, 1998.
- Hallquist, M., Wenger, J. C., Baltensperger, U., Rudich, Y., Simpson, D., Claeys, M., Dommen, J., Donahue, N. M., George, C., Goldstein, A. H., Hamilton, J. F., Herrmann, H., Hoffmann, T., Iinuma, Y., Jang, M., Jenkin, M. E., Jimenez, J. L., Kiendler-Scharr, A., Maenhaut, W., McFiggans, G., Mentel, T. F., Monod, A., Prévôt, A. S. H., Seinfeld, J. H., Surratt, J. D., Szmigielski, R., and Wildt, J.: The formation, properties and impact of secondary organic aerosol: current and emerging issues, *Atmospheric Chemistry and Physics*, 9, 5155–5236, <https://doi.org/10.5194/acp-9-5155-2009>, publisher: Copernicus GmbH, 2009.
- Hansen, J. C., Woolwine III, W. R., Bates, B. L., Clark, J. M., Kuprov, R. Y., Mukherjee, P., Murray, J. A., Simmons, M. A., Waite, M. F., Eatough, N. L., Eatough, D. J., Long, R., and Grover, B. D.: Semicontinuous PM_{2.5} and PM₁₀ Mass and Composition Measurements in Lindon, Utah, during Winter 2007, *Journal of the Air & Waste Management Association*, 60, 346–355, <https://doi.org/10.3155/1047-3289.60.3.346>, publisher: Taylor & Francis _eprint: <https://doi.org/10.3155/1047-3289.60.3.346>, 2010.
- Herckes, P., Valsaraj, K. T., and Collett, J. L.: A review of observations of organic matter in fogs and clouds: Origin, processing and fate, *Atmospheric Research*, 132–133, 434–449, <https://doi.org/10.1016/j.atmosres.2013.06.005>, 2013.
- Hrdina, A., Murphy, J. G., Hallar, A. G., Lin, J. C., Moravek, A., Bares, R., Petersen, R. C., Franchin, A., Middlebrook, A. M., Goldberger, L., Lee, B. H., Baasandorj, M., and Brown, S. S.: The role of coarse aerosol particles as a sink of HNO₃ in wintertime pollution events in the Salt Lake Valley, *Atmospheric Chemistry and Physics*, 21, 8111–8126, <https://doi.org/10.5194/acp-21-8111-2021>, publisher: Copernicus GmbH, 2021.
- Jimenez, J. L., Canagaratna, M. R., Donahue, N. M., Prevot, A. S. H., Zhang, Q., Kroll, J. H., DeCarlo, P. F., Allan, J. D., Coe, H., Ng, N. L., Aiken, A. C., Docherty, K. S., Ulbrich, I. M., Grieshop, A. P., Robinson, A. L., Duplissy, J., Smith, J. D., Wilson, K. R., Lanz, V. A., Hueglin, C., Sun, Y. L., Tian, J., Laaksonen, A., Raatikainen, T., Rautiainen, J., Vaattovaara, P., Ehn, M., Kulmala, M., Tomlinson, J. M., Collins, D. R., Cubison, M. J., E., Dunlea, J., Huffman, J. A., Onasch, T. B., Alfarra, M. R., Williams, P. I., Bower, K., Kondo, Y., Schneider, J., Drewnick, F., Borrmann, S., Weimer, S., Demerjian, K., Salcedo, D., Cottrell, L., Griffin, R., Takami, A., Miyoshi, T., Hatakeyama, S., Shimojo, A., Sun, J. Y., Zhang, Y. M., Dzepina, K., Kimmel, J. R., Sueper, D., Jayne, J. T., Herndon, S. C., Trimborn, A. M., Williams, L. R., Wood, E. C., Middlebrook, A. M., Kolb, C. E., Baltensperger, U., and Worsnop, D. R.: Evolution of Organic Aerosols in the Atmosphere, *Science*, 326, 1525–1529, <https://doi.org/10.1126/science.1180353>, 2009.
- Kanakidou, M., Myriokefalitakis, S., Daskalakis, N., Fanourgakis, G., Nenes, A., Baker, A. R., Tsigaridis, K., and Mihalopoulos, N.: Past, Present and Future Atmospheric Nitrogen Deposition, *Journal of the atmospheric sciences*, 73, 2039–2047, <https://doi.org/10.1175/JAS-D-15-0278.1>, 2016.
- Khemani, L. T., Momin, G. A., Naik, M. S., Rao, P. S. P., Safai, P. D., and Murty, A. S. R.: Influence of alkaline particulates on pH of cloud and rain water in India, *Atmospheric Environment (1967)*, 21, 1137–1145, [https://doi.org/10.1016/0004-6981\(87\)90241-1](https://doi.org/10.1016/0004-6981(87)90241-1), 1987.
- Khawaja, H. A., Brudnoy, S., and Husain, L.: Chemical characterization of three summer cloud episodes at whiteface mountain, *Chemosphere*, 31, 3357–3381, [https://doi.org/10.1016/0045-6535\(95\)00187-D](https://doi.org/10.1016/0045-6535(95)00187-D), 1995.
- Kiehl, J. T. and Briegleb, B. P.: The Relative Roles of Sulfate Aerosols and Greenhouse Gases in Climate Forcing, *Science*, 260, 311–314, <https://doi.org/10.1126/science.260.5106.311>, 1993.
- Kim, H., Collier, S., Ge, X., Xu, J., Sun, Y., Jiang, W., Wang, Y., Herckes, P., and Zhang, Q.: Chemical processing of water-soluble species and formation of secondary organic aerosol in fogs, *Atmospheric Environment*, 200, 158–166, <https://doi.org/10.1016/j.atmosenv.2018.11.062>, tex.ids= kimChemicalProcessingWatersoluble2019, kimChemicalProcessingWatersoluble2019a publisher: Elsevier Limited, 2019.



- Kumar, R., Bhardwaj, P., Pfister, G., Drews, C., Honomichl, S., and D'Attilo, G.: Description and Evaluation of the Fine Particulate Matter Forecasts in the NCAR Regional Air Quality Forecasting System, *Atmosphere*, 12, 302, <https://doi.org/10.3390/atmos12030302>, number: 3 Publisher: Multidisciplinary Digital Publishing Institute, 2021.
- Lance, S., Zhang, J., Schwab, J. J., Casson, P., Brandt, R. E., Fitzjarrald, D. R., Schwab, M. J., Sicker, J., Lu, C.-H., Chen, S.-P., Yun, J., Freedman, J. M., Shrestha, B., Min, Q., Beauharnois, M., Crandall, B., Joseph, E., Brewer, M. J., Minder, J. R., Orłowski, D., Christiansen, A., Carlton, A. G., and Barth, M. C.: Overview of the CPOC Pilot Study at Whiteface Mountain, NY: Cloud Processing of Organics within Clouds (CPOC), *Bulletin of the American Meteorological Society*, 101, E1820–E1841, <https://doi.org/10.1175/BAMS-D-19-0022.1>, publisher: American Meteorological Society Section: Bulletin of the American Meteorological Society, 2020.
- Lawrence, G. B. and David, M. B.: Response of Aluminum Solubility to Elevated Nitrification in Soil of a Red Spruce Stand in Eastern Maine, *Environmental Science & Technology*, 31, 825–830, <https://doi.org/10.1021/es960515j>, 1997.
- Lee, D. S. and Pacyna, J. M.: An industrial emissions inventory of calcium for Europe, *Atmospheric Environment*, 33, 1687–1697, [https://doi.org/10.1016/S1352-2310\(98\)00286-6](https://doi.org/10.1016/S1352-2310(98)00286-6), 1999.
- Liu, L., Zhang, X., Wong, A. Y. H., Xu, W., Liu, X., Li, Y., Mi, H., Lu, X., Zhao, L., Wang, Z., Wu, X., and Wei, J.: Estimating global surface ammonia concentrations inferred from satellite retrievals, *Atmospheric Chemistry and Physics*, 19, 12 051–12 066, <https://doi.org/https://doi.org/10.5194/acp-19-12051-2019>, 2019.
- Mahowald, N., Albani, S., Kok, J. F., Engelstaeder, S., Scanza, R., Ward, D. S., and Flanner, M. G.: The size distribution of desert dust aerosols and its impact on the Earth system, *Aeolian Research*, 15, 53–71, <https://doi.org/10.1016/j.aeolia.2013.09.002>, 2014.
- Marinoni, A., Laj, P., Sellegri, K., and Mailhot, G.: Cloud chemistry at the Puy de Dôme: variability and relationships with environmental factors, *Atmospheric Chemistry and Physics*, 4, 715–728, <https://doi.org/10.5194/acp-4-715-2004>, publisher: Copernicus GmbH, 2004.
- McNeill, V. F.: Aqueous Organic Chemistry in the Atmosphere: Sources and Chemical Processing of Organic Aerosols, *Environmental Science & Technology*, 49, 1237–1244, <https://doi.org/10.1021/es5043707>, 2015.
- Mekis, E., Donaldson, N., Reid, J., Zucconi, A., Hoover, J., Li, Q., Nitu, R., and Melo, S.: An Overview of Surface-Based Precipitation Observations at Environment and Climate Change Canada, *Atmosphere-Ocean*, 56, 71–95, <https://doi.org/10.1080/07055900.2018.1433627>, publisher: Taylor & Francis _eprint: <https://doi.org/10.1080/07055900.2018.1433627>, 2018.
- Mohnen, V. A.: Cloud water collection from aircraft, *Atmos. Technol.; (United States)*, 12, <https://www.osti.gov/biblio/6320448-cloud-water-collection-from-aircraft>, institution: State Univ. of New York, Albany, 1980.
- Mohnen, V. A. and Vong, R. J.: A climatology of cloud chemistry for the eastern United States derived from the mountain cloud chemistry project, *Environmental Reviews*, 1, 38–54, <https://www.jstor.org/stable/envirevi.1.1.38>, publisher: Canadian Science Publishing, 1993.
- Moore, K. F., Eli Sherman, D., Reilly, J. E., Hannigan, M. P., Lee, T., and Collett, J. L.: Drop size-dependent chemical composition of clouds and fogs. Part II: Relevance to interpreting the aerosol/trace gas/fog system, *Atmospheric Environment*, 38, 1403–1415, <https://doi.org/10.1016/j.atmosenv.2003.12.014>, tex.ids= mooreDropSizedependentChemical2004, 2004.
- Myhre, G., Shindell, D., Bréon, F.-M., Collins, W., Fuglestedt, J., Huang, J., Koch, D., Lamarque, J.-F., Lee, D., Mendoza, B., Nakajima, T., Robock, A., Stephens, G., Zhang, H., Aamaas, B., Boucher, O., Dalsøren, S. B., Daniel, J. S., Forster, P., Granier, C., Haigh, J., Hodnebrog, O., Kaplan, J. O., Marston, G., Nielsen, C. J., O'Neill, B. C., Peters, G. P., Pongratz, J., Ramaswamy, V., Roth, R., Rotstayn, L., Smith, S. J., Stevenson, D., Vernier, J.-P., Wild, O., Young, P., Jacob, D., Ravishankara, A. R., and Shine, K.: Anthropogenic and Natural Radiative Forcing, *Assessment Report of the Intergovernmental Panel on Climate Change*, 5, 82, 2013.
- Pachon, J. E., Weber, R. J., Zhang, X., Mulholland, J. A., and Russell, A. G.: Revising the use of potassium (K) in the source apportionment of PM_{2.5}, *Atmospheric Pollution Research*, 4, 14–21, <https://doi.org/10.5094/APR.2013.002>, 2013.



- Paerl, H. W. and Otten, T. G.: Harmful cyanobacterial blooms: causes, consequences, and controls, *Microbial Ecology*, 65, 995–1010, <https://doi.org/10.1007/s00248-012-0159-y>, 2013.
- Pandis, S. N. and Seinfeld, J. H.: Should bulk cloudwater or fogwater samples obey Henry's law?, *Journal of Geophysical Research: Atmospheres*, 96, 10 791–10 798, <https://doi.org/10.1029/91JD01031>, <https://agupubs.onlinelibrary.wiley.com/doi/pdf/10.1029/91JD01031>, 1991.
- 710 Pope, A. and Dockery, D. W.: Health Effects of Fine Particulate Air Pollution: Lines that Connect, *Journal of the Air & Waste Management Association*, 56, 709–742, <https://doi.org/10.1080/10473289.2006.10464485>, 2006.
- Popovich, N. and Katz, J.: See How Wildfire Smoke Spread Across America, *The New York Times*, <https://www.nytimes.com/interactive/2021/07/21/climate/wildfire-smoke-map.html>, 2021.
- 715 Pye, H. O. T., Nenes, A., Alexander, B., Ault, A. P., Barth, M. C., Clegg, S. L., Collett Jr., J. L., Fahey, K. M., Hennigan, C. J., Herrmann, H., Kanakidou, M., Kelly, J. T., Ku, I.-T., McNeill, V. F., Riemer, N., Schaefer, T., Shi, G., Tilgner, A., Walker, J. T., Wang, T., Weber, R., Xing, J., Zaveri, R. A., and Zuend, A.: The acidity of atmospheric particles and clouds, *Atmospheric Chemistry and Physics*, 20, 4809–4888, <https://doi.org/https://doi.org/10.5194/acp-20-4809-2020>, publisher: Copernicus GmbH, 2020.
- Rattigan, O. V., Civerolo, K. L., and Felton, H. D.: Trends in wet precipitation, particulate, and gas-phase species in New York State, *Atmospheric Pollution Research*, 8, 1090–1102, <https://doi.org/10.1016/j.apr.2017.04.007>, 2017.
- 720 Sander, R.: Compilation of Henry's law constants (version 4.0) for water as solvent, *Atmospheric Chemistry and Physics*, 15, 4399–4981, <https://doi.org/10.5194/acp-15-4399-2015>, 2015.
- Schwab, J. J., Casson, P., Brandt, R., Husain, L., Dutkewicz, V., Wolfe, D., Demerjian, K. L., Civerolo, K. L., Rattigan, O. V., Felton, H. D., and Dukett, J. E.: Atmospheric Chemistry Measurements at Whiteface Mountain, NY: Cloud Water Chemistry, Precipitation
725 Chemistry, and Particulate Matter, *Aerosol and Air Quality Research*, 16, 841–854, <https://doi.org/10.4209/aaqr.2015.05.0344>, [tex.ids=schwabAtmosphericChemistryMeasurements2016](https://doi.org/10.4209/aaqr.2015.05.0344) publisher: Taiwan Association for Aerosol Research, 2016a.
- Schwab, J. J., Wolfe, D., Casson, P., Brandt, R., Demerjian, K. L., Husain, L., Dutkewicz, V. A., Civerolo, K. L., and Rattigan, O. V.:
Atmospheric Science Research at Whiteface Mountain, NY: Site Description and History, *Aerosol and Air Quality Research*, 16, 827–
840, <https://doi.org/10.4209/aaqr.2015.05.0343>, 2016b.
- 730 Seinfeld, J. H. and Pandis, S. N.: *Atmospheric Chemistry and Physics: From Air Pollution to Climate Change*, Wiley, 3 edn., 2016.
- Sen, P. K.: Estimates of the Regression Coefficient Based on Kendall's Tau, *Journal of the American Statistical Association*, 63, 1379–1389, <https://doi.org/10.2307/2285891>, 1968.
- Simoneit, B. R. T.: Biomass burning — a review of organic tracers for smoke from incomplete combustion, *Applied Geochemistry*, 17, 129–162, [https://doi.org/10.1016/S0883-2927\(01\)00061-0](https://doi.org/10.1016/S0883-2927(01)00061-0), 2002.
- 735 Stevens, C. J., David, T. I., and Storkey, J.: Atmospheric nitrogen deposition in terrestrial ecosystems: Its impact on plant communities and consequences across trophic levels, *Functional Ecology*, 32, 1757–1769, <https://doi.org/https://doi.org/10.1111/1365-2435.13063>, <https://besjournals.onlinelibrary.wiley.com/doi/pdf/10.1111/1365-2435.13063>, 2018.
- Straub, D. J.: Radiation fog chemical composition and its temporal trend over an eight year period, *Atmospheric Environment*, 148, 49–61, <https://doi.org/10.1016/j.atmosenv.2016.10.031>, 2017.
- 740 Team, R. C.: R: A language and environment for statistical computing., <https://www.R-project.org/>, 2021.
- Tian, D. and Niu, S.: A global analysis of soil acidification caused by nitrogen addition, *Environmental Research Letters*, 10, 024 019, <https://doi.org/10.1088/1748-9326/10/2/024019>, 2015.
- US EPA, O.: Air Pollutant Emissions Trends Data, <https://www.epa.gov/air-emissions-inventories/air-pollutant-emissions-trends-data>, 2019.



- 745 Van Stempvoort, D. and Biggar, K.: Potential for bioremediation of petroleum hydrocarbons in groundwater under cold climate conditions: A review, *Cold Regions Science and Technology*, 53, 16–41, <https://doi.org/10.1016/j.coldregions.2007.06.009>, 2008.
- VandenBoer, T. C., Petroff, A., Markovic, M. Z., and Murphy, J. G.: Size distribution of alkyl amines in continental particulate matter and their online detection in the gas and particle phase, *Atmos. Chem. Phys.*, <https://doi.org/10.5194/acp-11-4319-2011>, 2011.
- van Pinxteren, D., Fomba, K. W., Mertes, S., Müller, K., Spindler, G., Schneider, J., Lee, T., Collett, J. L., and Herrmann, H.: Cloud water composition during HCCT-2010: Scavenging efficiencies, solute concentrations, and droplet size dependence of inorganic ions and dissolved organic carbon, *Atmospheric Chemistry and Physics*, 16, 3185–3205, <https://doi.org/10.5194/acp-16-3185-2016>, 2016.
- 750 Wang, Z., Mora Ramirez, M., Dadashazar, H., MacDonald, A. B., Crosbie, E., Bates, K. H., Coggon, M. M., Craven, J. S., Lynch, P., Campbell, J. R., Azadi Aghdam, M., Woods, R. K., Jonsson, H., Flagan, R. C., Seinfeld, J. H., and Sorooshian, A.: Contrasting cloud composition between coupled and decoupled marine boundary layer clouds, *Journal of Geophysical Research: Atmospheres*, 121, 11,679–11,691, <https://doi.org/10.1002/2016JD025695>, eprint: <https://onlinelibrary.wiley.com/doi/pdf/10.1002/2016JD025695>, 2016.
- 755 Warner, J. X., Dickerson, R. R., Wei, Z., Strow, L. L., Wang, Y., and Liang, Q.: Increased atmospheric ammonia over the world’s major agricultural areas detected from space, *Geophysical Research Letters*, 44, 2875–2884, <https://doi.org/10.1002/2016GL072305>, 2017.
- Winiwarter, W., Fierlinger, H., Puxbaum, H., Facchini, M. C., Arends, B. G., Fuzzi, S., Schell, D., Kaminski, U., Pahl, S., Schneider, T., Berner, A., Solly, I., and Kruisz, C.: Henry’s law and the behavior of weak acids and bases in fog and cloud, *Journal of Atmospheric Chemistry*, 19, 173–188, <https://doi.org/10.1007/BF00696588>, 1994.
- 760 Xie, S., Qi, L., and Zhou, D.: Investigation of the effects of acid rain on the deterioration of cement concrete using accelerated tests established in laboratory, *Atmospheric Environment*, 38, 4457–4466, <https://doi.org/10.1016/j.atmosenv.2004.05.017>, 2004.
- Zhang, F., Yu, X., Sui, X., Chen, J., Zhu, Z., and Yu, X.-Y.: Evolution of aqSOA from the Air–Liquid Interfacial Photochemistry of Glyoxal and Hydroxyl Radicals, *Environmental Science & Technology*, 53, 10 236–10 245, <https://doi.org/10.1021/acs.est.9b03642>, 2019.
- 765 Zhou, S., Collier, S., Jaffe, D. A., Briggs, N. L., Hee, J., Sedlacek III, A. J., Kleinman, L., Onasch, T. B., and Zhang, Q.: Regional influence of wildfires on aerosol chemistry in the western US and insights into atmospheric aging of biomass burning organic aerosol, *Atmospheric Chemistry and Physics*, 17, 2477–2493, <https://doi.org/10.5194/acp-17-2477-2017>, publisher: Copernicus GmbH, 2017.